water

MDPI

*Article*

# Effects of Climatic Drivers and Teleconnections on Late 20th Century Trends in Spring Freshet of Four Major Arctic-Draining Rivers

**Roxanne Ahmed [1], Terry Prowse [1,2], Yonas Dibike [1,2,*] and Barrie Bonsal [1,3]**

[1] Department of Geography, Water and Climate Impacts Research Centre, University of Victoria, P.O. Box 1700 STN CSC, Victoria, BC V8W 2Y2, Canada; roxannea@uvic.ca (R.A.); prowset@uvic.ca (T.P.); barrie.bonsal@canada.ca (B.B.)
[2] Watershed Hydrology and Ecology Research Division, Environment and Climate Change Canada, University of Victoria, 2472 Arbutus Rd., Victoria, BC V8N 1V8, Canada
[3] Watershed Hydrology and Ecology Research Division, National Hydrology Research Centre, Environment and Climate Change Canada, Saskatoon, SK S7N 3H5, Canada
* Correspondence: yonas.dibike@canada.ca

**Abstract:** Spring freshet is the dominant annual discharge event in all major Arctic draining rivers with large contributions to freshwater inflow to the Arctic Ocean. Research has shown that the total freshwater influx to the Arctic Ocean has been increasing, while at the same time, the rate of change in the Arctic climate is significantly higher than in other parts of the globe. This study assesses the large-scale atmospheric and surface climatic conditions affecting the magnitude, timing and regional variability of the spring freshets by analyzing historic daily discharges from sub-basins within the four largest Arctic-draining watersheds (Mackenzie, Ob, Lena and Yenisei). Results reveal that climatic variations closely match the observed regional trends of increasing cold-season flows and earlier freshets. Flow regulation appears to suppress the effects of climatic drivers on freshet volume but does not have a significant impact on peak freshet magnitude or timing measures. Spring freshet characteristics are also influenced by El Niño-Southern Oscillation, the Pacific Decadal Oscillation, the Arctic Oscillation and the North Atlantic Oscillation, particularly in their positive phases. The majority of significant relationships are found in unregulated stations. This study provides a key insight into the climatic drivers of observed trends in freshet characteristics, whilst clarifying the effects of regulation versus climate at the sub-basin scale.

**Keywords:** Arctic; spring freshet; hydro-climatology; streamflow; teleconnections; atmospheric circulation

**Citation:** Ahmed, R.; Prowse, T.; Dibike, Y.; Bonsal, B. Effects of Climatic Drivers and Teleconnections on Late 20th Century Trends in Spring Freshet of Four Major Arctic-Draining Rivers. *Water* **2021**, *13*, 179. https://doi.org/10.3390/w13020179

Received: 10 November 2020
Accepted: 7 January 2021
Published: 13 January 2021



## 1. Introduction

The Arctic Ocean plays a critical role in the global hydrological cycle through import, export, storage and transformation of freshwater. Freshwater is delivered to the Arctic Ocean mainly through direct precipitation on the ocean surface, import of lower-salinity Pacific waters through the Bering Strait, and terrestrial river runoff [1–3]. Export of relatively fresh water from the ocean southwards into the northern North Atlantic Ocean through the Fram Strait and the Canadian Arctic Archipelago couples the Arctic hydrological system with the global thermohaline circulation, with subsequent effects on oceanic heat transport to northern latitudes [1,2,4,5]. Since the Arctic Ocean is largely an enclosed system, it is particularly sensitive to river discharge from northward-flowing Arctic rivers. In fact, river discharges provide as much as 50% or more of the freshwater influx to the Arctic Ocean [6]. A change in the freshwater budget of the Arctic Ocean can alter the mechanisms of freshwater export and deep oceanic convection in the North Atlantic,

with resulting impacts on the thermohaline circulation [7,8]. In Arctic-draining rivers, as much as 60% of total annual flow volume is released during the spring freshet [9]. This annual event follows the spring snowmelt and river ice breakup period and is the major hydrologic event occurring on largely nival Arctic river systems.

Meanwhile, climate change is occurring more rapidly in Arctic regions than other parts of the globe. A warming Arctic climate corresponds to an earlier freshet onset and higher winter flow from greater subsurface infiltration into thawing permafrost. Additionally, northward redistribution of precipitation, increased sea ice melting, glacial wastage, permafrost degradation and an expected increase in river discharge may result in an intensification of the arctic hydrologic cycle. A growing number of studies point to changes in Arctic Ocean freshwater influx and distribution over recent periods [10,11]. For example, one investigation found that Eurasian river discharge had increased by approximately 7% over the period 1936–1999 [4]. This amounted to a volumetric increase of 128 $km^3$ of freshwater annually by the end of the study period, or an increase of 2.0 ± 0.7 $km^3$/year, and was correlated with trends in global surface air temperature and the North Atlantic Oscillation (NAO). Another study described a rapid change in the freshwater content in the western portion of the Arctic Ocean where freshwater had increased by 8500 $km^3$, or 26%, compared to winter climatological values. River runoff and increased precipitation were amongst the dominant sources of the increase [12].

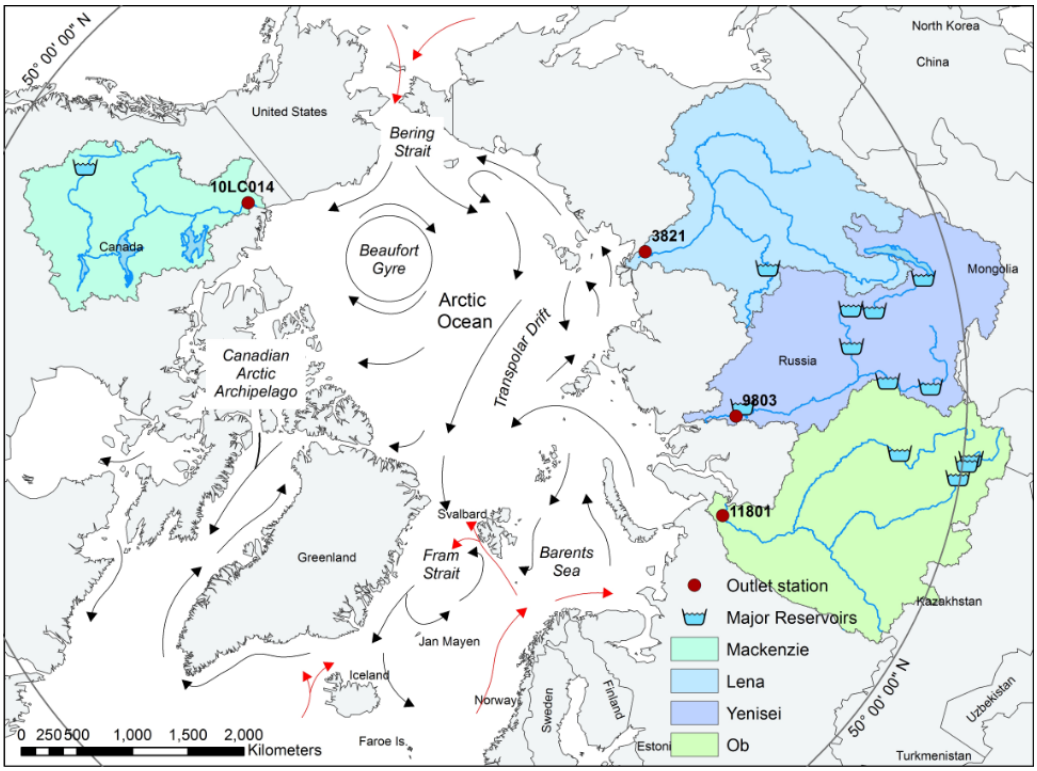


**Figure 1.** Map showing the Arctic Ocean, ocean features, major surface currents, and drainage basins and outlet stations of the Mackenzie, Ob, Lena and Yenisei (MOLY) rivers. Red arrows denote warmer currents, while black arrows denote colder currents. Figure adapted from Figure 6 in [8].

In the current state of changing Arctic climate, there is a need to better understand climate-discharge relationships in Arctic river systems, particularly in the four largest Arctic-draining rivers: the Mackenzie River in North America, and the Ob, Lena and Yenisei rivers in Asia, hence referred to as MOLY (see Figure 1). Combined, these four rivers contribute almost 1900 $km^3$ of freshwater to the Arctic Ocean per year, or about 60% of annual flow volume from all Arctic contributing areas [6,13]. It was reported that the total annual freshwater influx from MOLY to the Arctic Ocean increased by 89 $km^3$/decade,

amounting to a 14% increase during the 30-year period from 1980 to 2009 [14,15]. Seasonality of discharge was also found to have shifted and the percentage of freshet discharge released as a fraction of annual flow actually decreased by 1.7% during the period 1980–2009, while winter, spring and fall all increased (1.3%, 2.5% and 2.5%', respectively). However, summer flows were reduced by 5.8%, indicating a shift toward earlier peak discharges. While this overall increase seems proportionally larger than earlier studies incorporating only major Eurasian basins, it was also noted that observed trends varied substantially depending on the analysis window utilized [14].

This study analyzes correlations of large scale atmospheric and surface climatic patterns to the spring freshet for 106 sub-basins located within the MOLY watersheds, and links changing seasonality and magnitude of outlet discharges to key hydro-climatic drivers. To separate the effects of flow regulation from that of climate, the sub-basins are classified based on regulation status and regional topography. This approach helps identify whether significant hydro-climatic relationships over regions unaffected by flow regulation have the potential to be major drivers of changes observed at the outlets, and whether climatic conditions leading to increased peak freshet magnitudes in regulated basins are also an important control.

## 2. Basin Characteristics and Climatic Patterns

### *2.1. Basin Physiography*

The pan-Arctic drainage areas of the MOLY rivers are shown in Figure 1, with detailed basins presented in Figure 2a–d. Total contributing areas of the four major river systems, including ungauged drainage areas, are as follows: Mackenzie 1,800,000 km$^2$ [16]; Ob 2,975,000 km$^2$ [17]; Lena 2,488,000 km$^2$ [18]; and Yenisei 2,554,482 km$^2$ [19]. The pan-Arctic region contains nearly half of the global alpine and sub-polar glacial area [20], while two of the four Arctic basins have a catchment area extending below 50° N, further south than what is traditionally considered the Arctic region [21] (see Figure 1). As a result, discharge behaviour at each of the four major drainage outlets is influenced along its course by sub-basin tributaries which may adhere to a variety of hydrological regimes such as nival, pluvial, wetland, proglacial, prolacustrine, regulated, hybrid or other. For example, hydrologic retention due to extensive wetland coverage or large lakes within a catchment, such as found in the Ob or Mackenzie basins, will lead to a more moderated seasonal discharge characteristic than basins without such retention, and spring floods in the Ob Basin may persist for up to 100 days [2,22].

The Mackenzie Basin encompasses topography typical of the North American Cordillera in the western sub-basins, interior plains along the central Mackenzie corridor, and Precambrian Canadian Shield in the eastern portion of the basin [23]. The Ob Basin covers a portion of the Altai Mountains, where its headwaters originate, although up to 85% of the basin is situated in the Western Siberian lowlands [22]. Central portions of the lowlands consist of taiga with extensive expanses of wetlands [24]. By contrast, the Yenisei comprises a greater proportion of mountainous terrain. Southern portions of the Yenisei Basin encompass the Western and Eastern Sayan mountain ranges as well as Lake Baikal, and up to 80% of the basin is located in the Central Siberian Plateau, with elevations ranging from 500–700 m a.s.l. The basin is bordered by the Yenisei Ridge in the west and the Putorana Mountains in the northeast [24]. The Lena Basin includes the Baikal Mountains in the south, Yakut Lowlands below the mouth of the Aldan tributary, and Verkhoyansk Mountains to the east [24]. A topographical map of the four basins showing sub-basins classification into Northern, Southern, Western and Eastern regions is shown on Figure 2c,d.

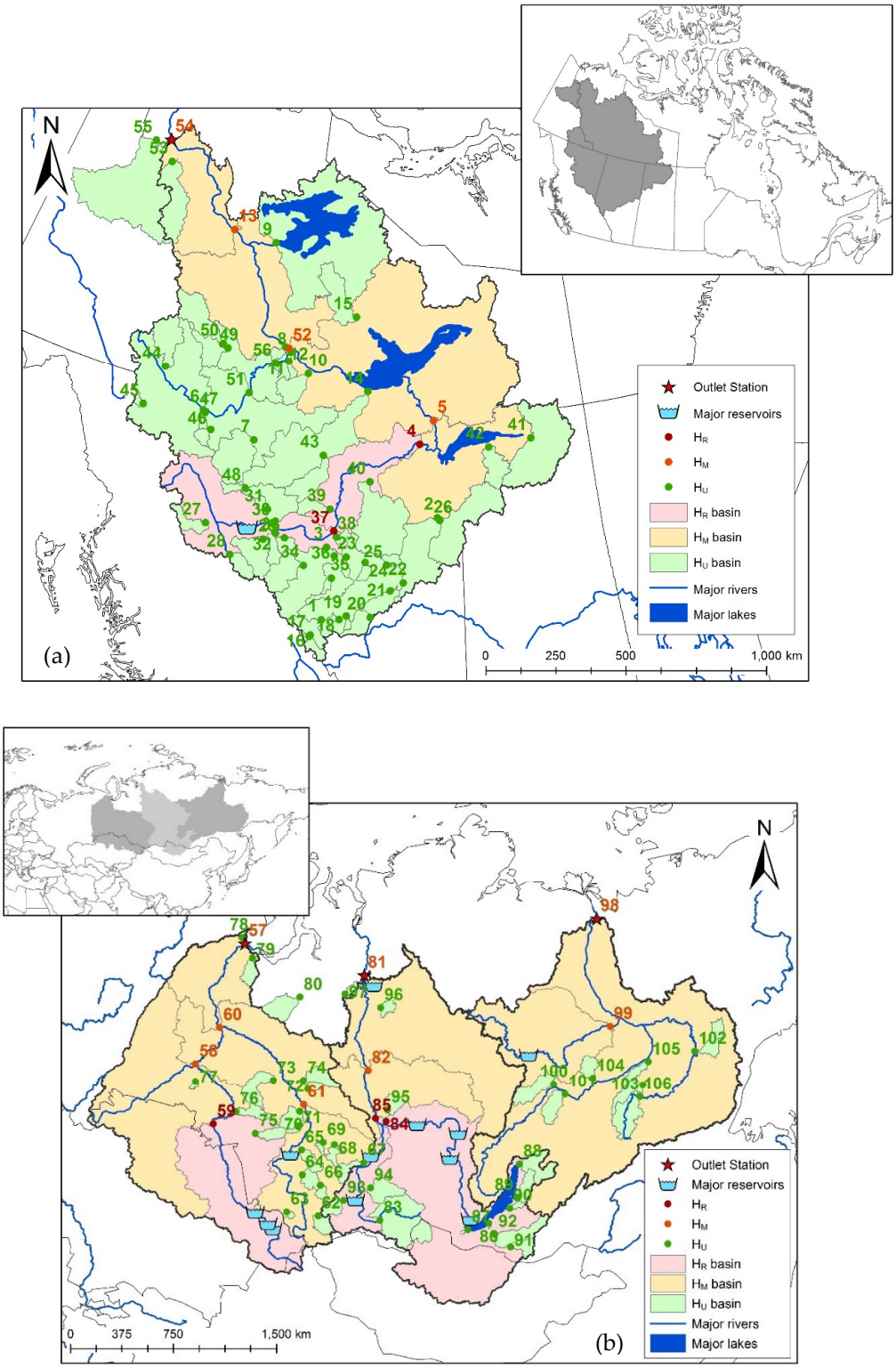
N
Outlet Station
Major reservoirs
$H_R$
$H_M$
$H_U$
$H_R$ basin
$H_M$ basin
$H_U$ basin
Major rivers
Major lakes
0 250 500 1,000 km
(a)
N
0 375 750 1,500 km
(b)

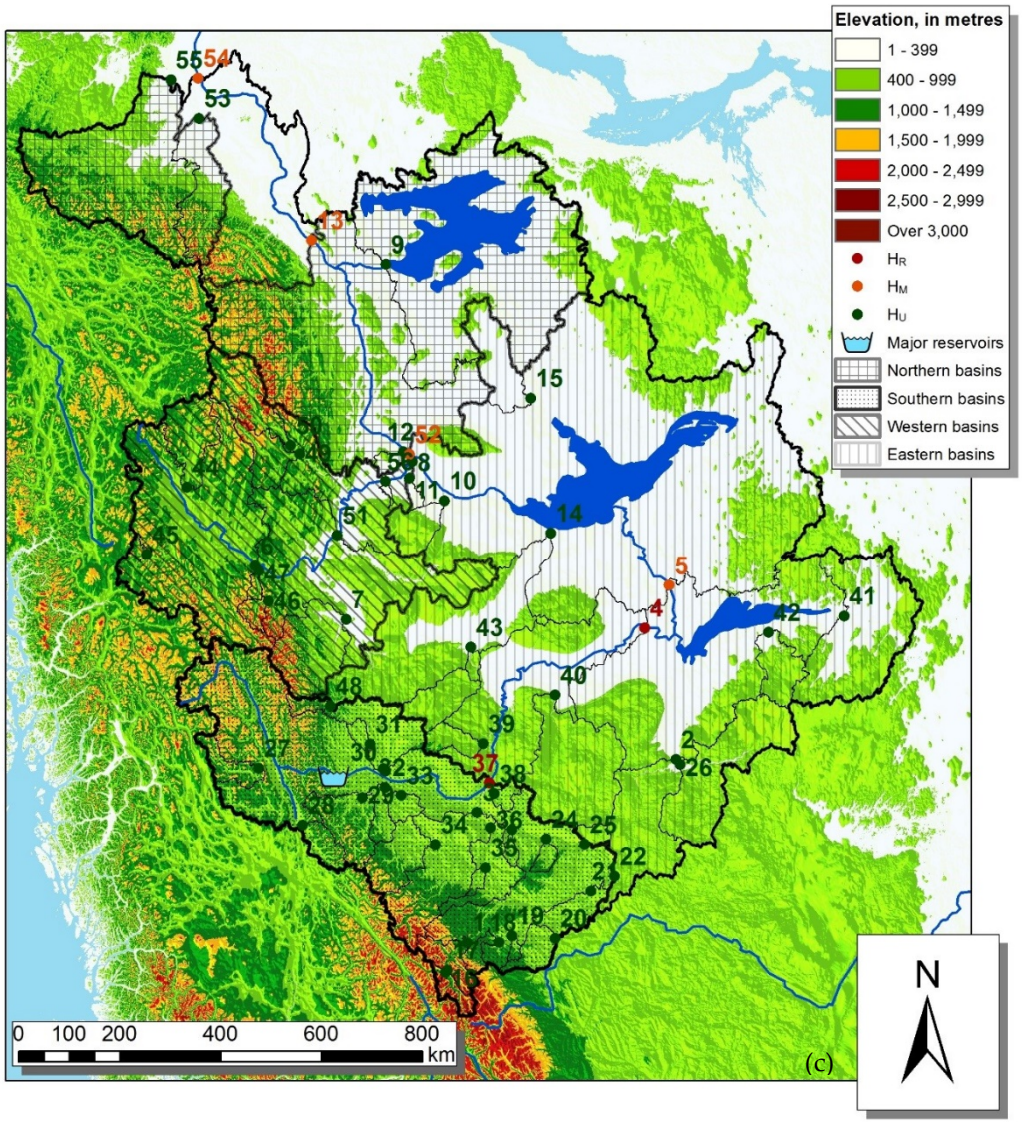
Elevation, in metres
1 - 399
400 - 999
1,000 - 1,499
1,500 - 1,999
2,000 - 2,499
2,500 - 2,999
Over 3,000
HR
HM
HU
Major reservoirs
Northern basins
Southern basins
Western basins
Eastern basins
0 100 200 400 600 800
km
N
(c)

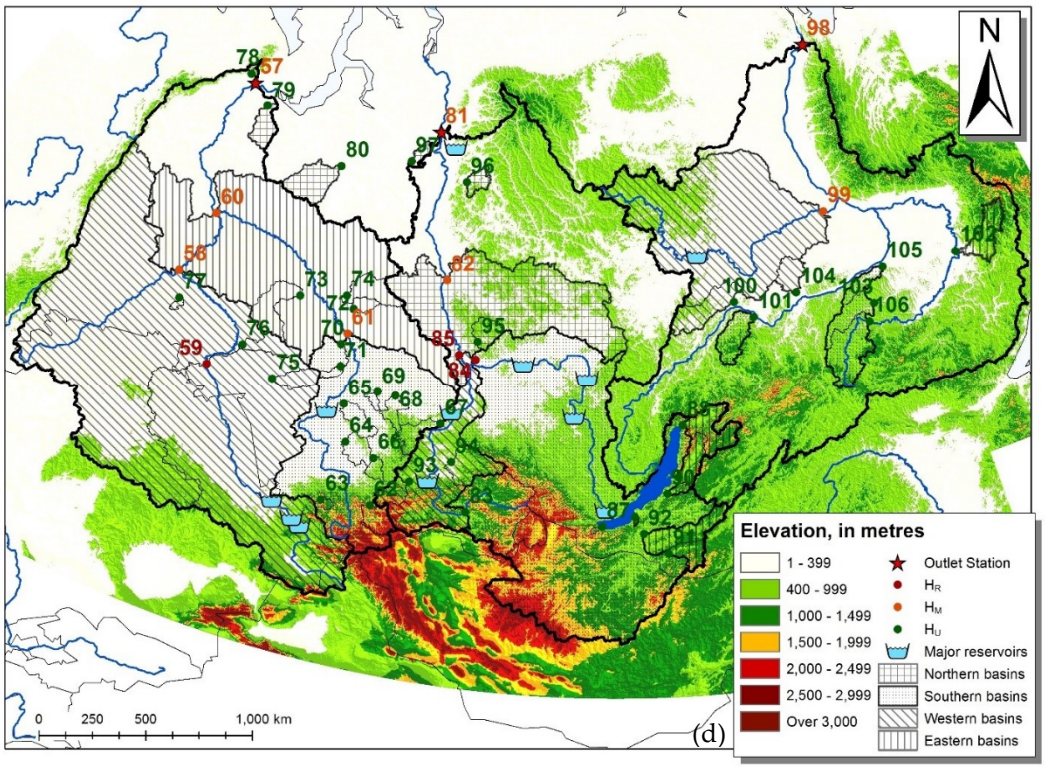


**Figure 2.** Study area of the (**a**) Mackenzie basin (**b**) Ob, Yenisei and Lena basins (left to right in the map) showing station and sub-basins color-coded and classified as regulated ($H_R$), minimally regulated ($H_M$) or unregulated ($H_U$). Topographical map of the (**c**) Mackenzie basin (**d**) Ob, Yenisei and Lena basins showing regional classification of sub-basins into Northern, Southern, Western and Eastern regions. Station descriptions are provided in Table S1 of the supplementary material.

### *2.2. Flow Regulation*

Each of the MOLY watersheds experiences some degree of flow regulation within their catchments. The Yenisei basin is the most substantially regulated, with at least six major reservoirs having a capacity greater than 25 km$^3$ located along the Yenisei and Angara stems [19,25]. The next most regulated is the Ob basin, containing one major reservoir with capacity greater than 25 km$^3$ and three midsize dams [17]. Of the Asian basins, the Lena is least affected by flow regulation, with only one major reservoir located along the Vilyuy tributary. The Mackenzie basin is also considered moderately affected, despite only one major reservoir located along the Peace River tributary. Large lakes in the Mackenzie basin (e.g., Great Slave and Great Bear Lakes) provide substantial natural storage capacity, acting to reduce high spring peaks and sustain lower flows resulting in a more consistent runoff pattern throughout the year, similar to the effect of flow regulation [23]. Percentage of area in each basin directly upstream of a major reservoir, obtained by delineating the drainage area of each major reservoir, is as follows: Mackenzie 3.9%; Ob 11.6%; Yenisei 46.5% and Lena 4.2%. Figures 1 and 2 show the locations of major reservoirs, while their characteristics are provided in Table 1.

**Table 1.** Characteristics of major hydroelectric dams/reservoirs located in the study regions.

| Reservoir/Dam Name | Latitude (°N) | Longitude (°E) | Basin | River | Capacity (MW) | Commis-sioned | Maximum Capacity (km³) | Catchment Area (km²) |
|---|---|---|---|---|---|---|---|---|
| W.A.C. Bennett | 56.0 | −122.2 | Mackenzie | Peace | 2730 | 1968 | 74 | 70,275 |
| Shul'binsk | 50.4 | 81.1 | Ob | Irtysh | 702 | 1969 | 2.4 | 131,598 |
| Bukhtarma | 49.7 | 83.3 | Ob | Irtysh | 750 | 1960 | 49.8 | 103,923 |
| Ust-Kamenogorsk | 49.9 | 82.7 | Ob | Irtysh | 331.2 | 1952 | 0.6 | 107,636 |
| Novosibirsk | 54.8 | 83.0 | Ob | Ob | 455 | 1957 | 8.8 | 212,076 |
| Boguchany | 58.4 | 97.4 | Yenisei | Angara | 3000 | 2011 | 58.2 | 845,694 |
| Ust-Ilimsk | 58.0 | 102.7 | Yenisei | Angara | 4320 | 1974 | 59.3 | 767,413 |
| Bratsk | 56.3 | 101.8 | Yenisei | Angara | 4500 | 1967 | 169 | 714,017 |
| Irkutsk | 52.2 | 104.3 | Yenisei | Angara | 662.4 | 1958 | 46 | 572,704 |
| Sayano-Shushenskoe | 52.8 | 91.4 | Yenisei | Yenisei | 6400 | 1978 | 31.3 | 172,529 |
| Krasnoyarskoye More | 55.9 | 92.3 | Yenisei | Yenisei | 6000 | 1972 | 73.3 | 276,174 |
| Kurejka | 66.9 | 88.3 | Yenisei | Kurejka | 600 | 1987 | - | 65,974 |
| Vilyuy | 63.0 | 112.5 | Lena | Vilyuy | 680 | 1967 | 35.9 | 104,566 |

- data not available.

### *2.3. Regional Climate*

The Mackenzie Basin covers several climatic regions, including cold temperate, mountain, subarctic and arctic zones with precipitation ranging from greater than 1000 mm in the southwest of the basin to only 200 mm in the delta region [23]. Mean surface air temperature (SAT) averaged over the entire basin is around −25 °C in January and 13.8 °C in July. Climate in the Ob Basin is characterized by a cold continental and subarctic to arctic climate. It is the warmest of the four basins, with a mean SAT of −18.7 °C in January and 18.1 °C in July. However, summer maximum temperatures in the arid south can reach 40 °C while winter temperatures in the Altai Mountains can fall as low as −60 °C. Precipitation, which falls mainly as rain during the summer, can reach up to 1575 mm annually in the Altai Mountains while much of the rest of the basin receives 300–600 mm annually [26]. Climate in the Yenisei Basin ranges from continental in the southern and central portions to subarctic in the north. Average winter temperatures range from −20 °C in the south to −32 °C in northern regions, while summer average temperatures range from 20 °C in the south to 12 °C in the north. Mean SAT is −26.5 °C in January and 15.2 °C in July. Precipitation, which falls chiefly as rain during the warmer months, ranges from 400–500 mm annually in the north, 500–750 mm in the central regions, and up to 1200 mm annually in the south [26]. Similarly, climate in the Lena Basin ranges from continental to subarctic and arctic. The Lena is the coldest of the four basins where winters are cold, clear and calm, with temperatures falling as low as −70 °C. Mean SAT in January is −35 °C and 14.7 °C in July. The southern mountain ranges receive up to 600–700 mm of precipitation annually, while the central basin receives 200–400 mm and 100 mm falls annually in the delta regions. Like the other basins, most precipitation falls as rain during the summer [24,26].

### *2.4. Teleconnection Patterns*

Relationships between various large-scale oceanic and atmospheric oscillations and freshet characteristics are explored using four teleconnection indices that have previously been shown to affect climate in the areas of interest: Arctic Oscillation (AO), North Atlantic Oscillation (NAO), Pacific Decadal Oscillation (PDO), and El Niño-Southern Oscillation (ENSO). ENSO is the leading pattern of interannual climate variability in the Pacific [27]. The PDO index is derived as the leading principal component of monthly sea surface temperature (SST) anomalies in the Pacific Ocean north of 20° N, separated from global

SST anomalies to distinguish the pattern from any climate warming signal [28]. The AO is defined as the leading principal component of sea level pressure (SLP) anomalies north of 20° N and varies considerably in intra-seasonal time scales in mid to high-latitudes [29]. The NAO is the normalized difference in surface pressure (SP) between stations in Azores and Iceland [30]. In Canada, freshwater trends and variability have been linked to phases of the AO, ENSO and PDO [31]. For example, stronger positive phases of the PDO and ENSO have been shown to be a factor in decreased precipitation and, subsequently, decreased river discharge in northern Canada [32] while PDO in particular has been shown to affect hydrologic variability in western North American regions which may be encompassed by the Mackenzie basin [33,34]. El Niño conditions and positive phases of PDO are representative of a deeper Aleutian Low, which has been linked to warmer winter and spring temperatures and, subsequently, earlier snowmelt and freshwater ice break-up events in Western Canada [31]. The opposite tendencies are associated with La Niña/negative phases of PDO.

On the other hand, spring river discharge in the three Asian basins has been positively correlated with winter and spring AO, an effect likely due to a high correlation of spring air temperature with the AO [35]. The AO has a strong center of action over the central Arctic Ocean but displays weaker centers of opposing sign over the northern Atlantic and northern Pacific oceans [36], thus exhibiting a weaker influence on climatic conditions over those regions. The positive phase of the AO results in anomalously high sea-level pressure in the mid-latitudes and lower pressure in the Arctic, causing confinement of cold air to the Arctic and resulting in warmer Northern Hemisphere winters [37]. Positive indices of NAO are representative of a stronger Icelandic Low, leading to colder winters and springs (and hence later freshwater break-up dates) over western Atlantic regions and vice versa [30,31]. Like the AO, the NAO is most active in winter months, bringing cold, dry Arctic air over northern Canada during its positive phase [38]. Although the NAO and AO are highly correlated and nearly identical in the temporal domain, with both demonstrating similar structures [29], there is evidence of distinct regional differences [39]. For example, effects of the NAO tend to be regionalized while AO effects are on a more global scale [40], with the NAO in particular being shown to affect variability in temperature and precipitation over the Northern Hemisphere [30]. Thus, both indices are included in this study to assess any potential regional differences.

## 3. Data and Methods

### *3.1. Data Sources*

Daily discharge data for stations in the Mackenzie basin are obtained from the Environment and Climate Change Canada Hydrometric Database (HYDAT) while, for the Ob, Lena and Yenisei basins**,** discharge data are obtained from the Regional, Hydrometeorological Data Network for Russia (R-ArcticNET Russia v4.0) [41]. R-ArcticNET Russia (v4.0) contains information from 139 Russian Arctic gauges compiled from original archives of the State Hydrological Institute (SHI) and the Arctic and Antarctic Research Institute (AARI), St. Petersburg, Russia. Availability of hydrometric data is temporally limited, particularly in the Mackenzie region. As a result, two time periods are utilized to maximize the number of stations selected for inclusion: 1962–2000 and 1980–2000. These two periods are hence referred to as $t_1$ and $t_2$, respectively. Currently, the temporal range of Eurasian station data for most Lena, Yenisei and Ob sub-basins obtained from R-ArcticNET Russia (v4.0) does not extend past the year 2000, whilst many stations in the Mackenzie basin have incomplete or missing data in the period 1970–1979. Hence, the shorter period $t_2$ is chosen to maximize spatial coverage of stations with available data, while the longer period $t_1$ is used to increase the power of significance testing and t-tests for stations that had available data. All Asian sub-basin stations have data from 1962 or earlier and Table S1 identifies the stations in the Mackenzie region that have available data throughout both time periods. In total, there are 66 stations for $t_1$ and 106 stations for $t_2$ and the

relevant station information for all 106 stations is provided in Table S1 of the supplementary material.

Climate data for all the basins is derived from the Climatic Research Unit (CRU) Time-Series (TS) Version 3.21 (CRU TS3.21) covering the period January 1901–December 2012 [42]. CRU TS3.21 is a gridded climatic dataset constructed from monthly observations of global meteorological stations and has a spatial resolution of 0.5 × 0.5 degrees covering all global land areas, excluding Antarctica. Teleconnection indices for AO, NAO, PDO and ENSO are obtained from the National Oceanic and Atmospheric Administration (http://www.esrl.noaa.gov/psd/data/climateindices/list/) as monthly standardized anomalies. In this study the common Niño 3.4 index of SST anomalies is used to classify ENSO conditions, which capture the region bounded between 5° S–5° N and 170° W–120° W.

### *3.2. Sub-basin Classification*

To identify the effect of regulation, sub-basin stations have been classified into three categories. The first is unregulated stations ($H_U$) that are not impounded in their upstream catchment areas. These catchment areas are considered regionally representative of a natural, unregulated basin with stable hydrologic conditions. The second category is regulated stations ($H_R$) that are located downstream of a major reservoir and have seasonal runoff patterns that are strongly influenced by the upstream flow impoundment. The third category is that of minimally regulated stations ($H_M$) that correspond to stations with an upstream impounded flow signal that has been noticeably diminished by contribution from unaffected $H_U$ basins. However, such determination requires a comparison of the station's average hydrograph to that of an $H_R$-classified upstream station, and also to unaffected $H_U$-classified upstream contributing basins. One should also note that $H_U$ stations gauging the outlet of any large water body such as a natural lake will exhibit flow characteristics similar to that of an $H_R$ station. The assigned classifications of each of the 106 analyzed stations are given in Table S1 with their associated sub-basin drainage areas (also shown in Figure 2a,b). Approximately 85% of total gauged drainage area is classified as $H_U$ in the Mackenzie. Due to limited station availability and expansive flow regulation in the Asian basins, only 9% of gauged area is classified as $H_U$ in the Ob, 12% in the Yenisei and 8% in the Lena basin. Sub-basins are also classified using a simple characterization based on geography and topology. Sub-basins in each watershed are roughly divided into northern, southern, eastern and western regions of similar topographical composition (see Figures 2c,d).

### *3.3. Flow Estimation*

Missing data in the hydrometric records are estimated using three different techniques. If there is an available upstream or downstream station gauging along the same water course as the station with missing records, measurements from that gauge are used provided that it has a complete record over the period to be estimated. To account for any additional or reduced contributing area, the estimated river runoff rate is scaled up or down using Equation (1).

$$R_P = R_F A_P / A_F \quad (1)$$

where R denotes the runoff rate ($m^3/s$) over an area A ($m^2$) and subscripts P and F identify the partial and full records, respectively [32]. Similarly, stations with partial records that have no upstream or downstream station along the same tributary are assessed for areal runoff scaling by comparing the hydrologic response to the closest available basin, provided it has similar hydrologic characteristics. Whenever possible, missing records are assigned values from basins with similar morphology and scaled by basin area in the same fashion as Equation (1) [43]. If there are no suitable stations to use for runoff scaling, then missing discharge values are estimated from the mean daily value over the entire evaluated time period, adjusted by the deviation in discharge from the mean of all rivers in the larger basin (evaluated over the same time period) for which data are available on

the missing day [32]. At least three rivers, which do not have concurrent missing data, are used for reconstruction in all cases. Here, data are reconstructed according to Equation (2):

$$R_P = \frac{R_1 + R_2 + \cdots + R_N}{\overline{R_1} + \overline{R_2} + \cdots + \overline{R_N}} \times \overline{R_P} \quad (2)$$

where $R_P$ is the station with partial records for which missing data are to be reconstructed, $\overline{R_P}$ is the mean discharge for a specific day over the remaining time period, and $R_1 \ldots R_N$ and $\overline{R_1} \ldots \overline{R_N}$ are the time series of discharge for a particular day and the daily mean of the corresponding station for the evaluated time period, respectively. In total, 46 out of 106 stations required infilling techniques to estimate missing data for one or more days throughout their records. The percentages of missing data infilled for each station, where applicable, are given in Table S1 of the supplementary material.

### *3.4. Spring Freshet Definition*

Two methods are used to define the volume of discharge released during the spring freshet period: (i) flows occurring during the period April through July (AMJJ), referred to as $V_1$ and (ii) integrated flow from the date of the spring pulse onset to the hydrograph center of mass calculated from pulse onset to the last day of the calendar year, referred to as $V_2$. July is used as the end-date of the $V_1$ period since some basins display high discharge rates well into the summer months. The date of the spring pulse onset is determined as the date at which cumulative departure from mean annual flow is most negative. This yields the date when flows on subsequent days are greater than the year average [44,45]. Choosing the freshet end date by visual means is subjective and influenced by precipitation, temperature and other factors; therefore, the hydrograph center of mass, adjusted by pulse onset as the freshet end date, is used as a consistent method for determination of the freshet end date. All five metrics used to analyze freshet characteristics are listed in Table 2. Visual indicators of the pulse onset, freshet end date, peak magnitude and $V_1$ and $V_2$ definitions of the spring freshet for a sample year of the Yenisei River outlet station is provided in Figure 3.

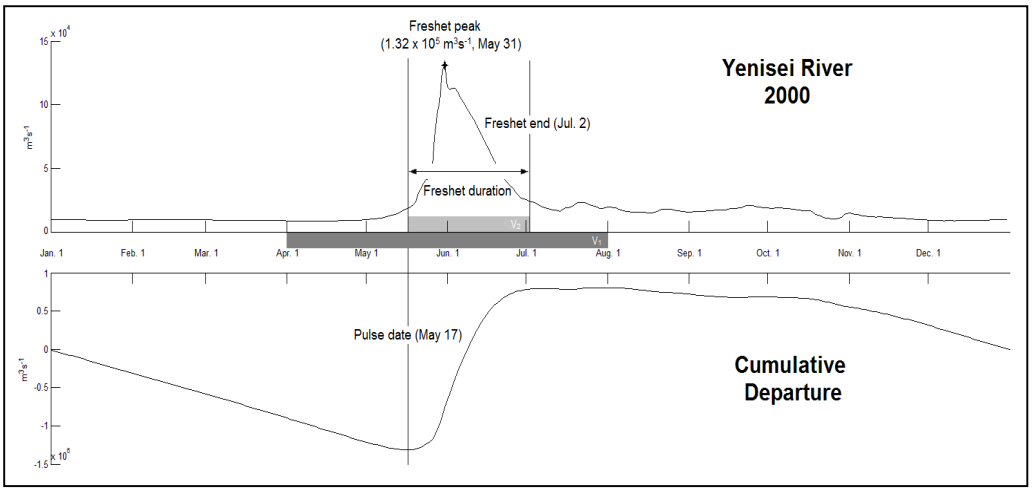


**Figure 3.** Illustration of freshet parameters using daily flow (top graph) and cumulative departure from mean flow (bottom graph) for the Yenisei River during the year 2000. The date at which cumulative departure is at a minimum defines the onset of the spring pulse ($F_P$). The freshet end date is defined as the annual hydrograph centre of mass date and the freshet duration ($F_L$) is the number of days between the freshet onset and the freshet end date where the freshet peak magnitude ($F_M$) is recorded. Shaded grey regions denote the time periods used to integrate flows occurring from April through July ($V_1$) and during freshet duration ($V_2$).

**Table 2.** The five freshet metrics used to describe freshet characteristics.

| Symbol | Description | Units |
|---|---|---|
| $F_P$ | Freshet pulse date | Julian day |
| $F_L$ | Freshet length | days |
| $F_M$ | Peak freshet magnitude | $m^3/s$ |
| $V_1$ | April–July volume | $m^3$ |
| $V_2$ | Freshet volume | $m^3$ |

### *3.5. Climatic Variation and Teleconnections*

A Pearson's *r* correlation analysis is used to examine the linear associations between climatic variables and spring freshet discharge. Significant correlations are indicated at the 5% and 10% levels. For each sub-basin, climatic correlations are obtained for pulse dates $F_P$, freshet lengths $F_L$, and peak freshet magnitudes $F_M$ with temperature, and freshet volumes $V_2$ and April–July volumes $V_1$ with precipitation. Correlations are computed using the spatial average of the climatic variable over the respective sub-basin. Temperatures are averaged over April–June for climatic correlations with $F_P$, $F_L$ and $F_M$ since these measures may be affected by climatic conditions just prior to or during the spring breakup period. However, volume measures may be affected by previous seasonal conditions, so to accommodate for seasonal lag of accumulated precipitation the period of November is chosen for climatic correlations of cumulative precipitation with $V_1$ and $V_2$.

Teleconnection indices are averaged into a "spring" season of March–May and a "winter" season of December–February, to accommodate for influence of both current and lagged previous-season atmospheric/oceanic conditions. The winter season teleconnection indices are used for precipitation-related variables while the spring season teleconnection indices are used for temperature-related variables. Since climate signals from large-scale teleconnections are not always linearly related to the hydro-climatic variable (i.e., a strong relationship may exist in one phase but may be weak or non-existent in the other), a composite approach is used to assess potential relationships between freshet characteristics and teleconnection patterns [46,47]. The scatterplot of Figure 4 illustrates an example of this, in which the ten highest and ten lowest NAO values are averaged over December–February and plotted against freshet volume for station 07NB001 (No. 5 in Figure 2). Here, the relationship is clearly stronger for positive values of the NAO index, but weaker for negative values. For this analysis, freshet statistics for years corresponding to the top/bottom 25% of teleconnection indices for each time period are evaluated separately. This provides 10 and 5 values in each group for t1 and t2, respectively, and a t-test is conducted to determine if the mean of each set is significantly different (at a 5% significance level) from the entire series mean.

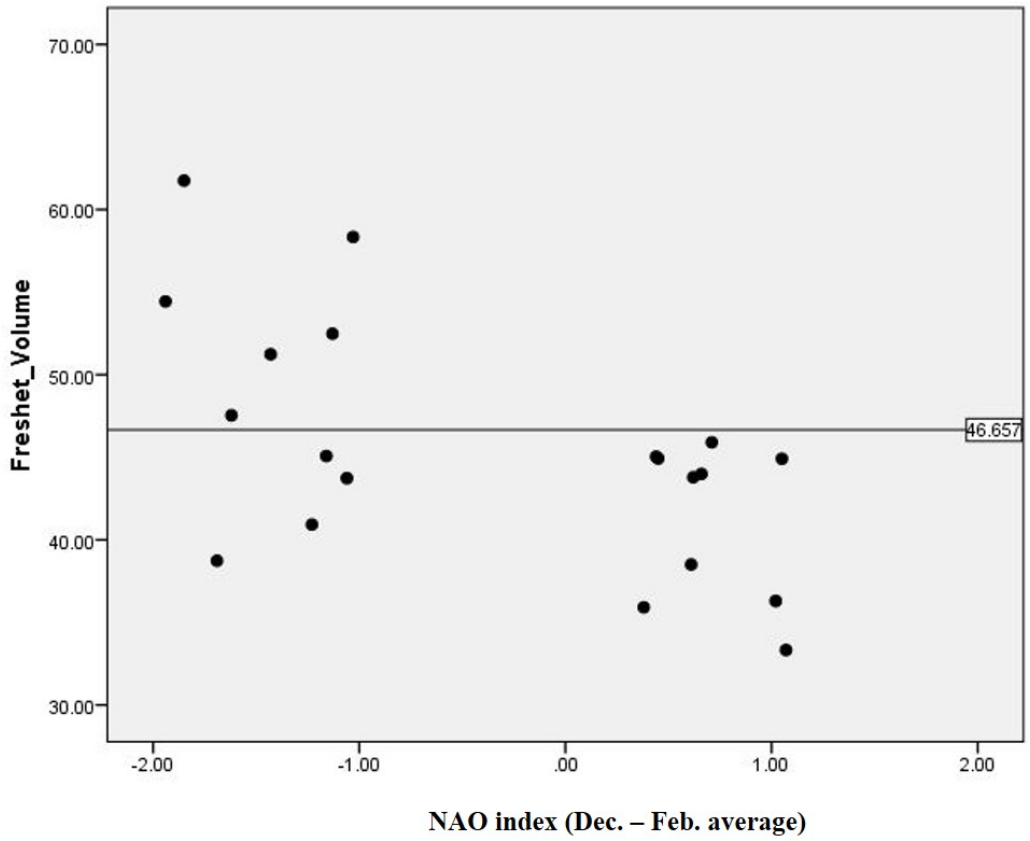


**Figure 4.** Scatterplot of the ten highest and ten lowest NAO December–February average values against freshet volume for station 07NB001 in the Mackenzie basins (No. 5 in Figure 2) during the 1962–2000 period. Horizontal line denotes mean freshet volume for the period.

## 4. Results and Discussion

### *4.1. Effect of Climatic Drivers*

Strength and significance of correlations of climatic variables with freshet measures for the periods 1962–2000 and 1980–2000 ($t_1$ and $t_2$, respectively) are shown in Figures 5–9. Figure 5 displays the correlations of average April–June temperatures with freshet pulse dates $F_P$ during $t_1$ and $t_2$ for the Mackenzie and Asian basins. A negative correlation indicates that warmer April–June temperatures are correlated with earlier pulse dates, and vice versa. During both time periods, correlations are overwhelmingly moderately to strongly negative and significant at the 5% level in all four basins. The most notable clustering of weak or negligible correlations resides in the southern portion of the Mackenzie basin and eastern Yenisei and is observed during both $t_1$ and $t_2$. Only one small-sized basin, 07AF002 (No. 18 in Figure 2) located in the southern portion of the Mackenzie basin, demonstrates a significant, positive correlation of warmer April–June temperature with later pulse dates for both time periods. At least 64% and up to 100% of all significant correlations with $F_P$ occur in unregulated stations ($H_U$, see Table 3), although some significant correlations are also seen in the regulated ($H_R$) Irtish (Ob), Angara (Ob) and Yenisei stems (not shown).

**Table 3.** Percentage of total significant correlations (5% level) between climatic variables and freshet measures (April–June mean temperature for $F_P$, $F_L$, $F_M$, and November–March precipitation for $V_2$ and $V_1$) occurring in unregulated ($H_U$) stations during the 1962–2000 ($t_1$) and 1980–2000 ($t_2$) period. Items marked by *N/A* indicate that there were no significant correlations for the corresponding freshet measure.

| River Basins | $F_P$ | | $F_L$ | | $F_M$ | | $V_2$ | | $V_1$ | |
|---|---|---|---|---|---|---|---|---|---|---|
| | $t_1$ | $t_2$ | $t_1$ | $t_2$ | $t_1$ | $t_2$ | $t_1$ | $t_2$ | $t_1$ | $t_2$ |
| Mackenzie | 100 | 88 | 88 | 91 | 80 | 100 | 92 | 83 | 86 | 71 |
| Ob | 78 | 76 | 57 | 100 | 63 | 100 | 75 | N/A | 100 | 100 |
| Lena | 75 | 71 | 50 | 0 | 100 | N/A | 100 | N/A | 100 | N/A |
| Yenisei | 64 | 67 | 50 | 67 | 50 | 100 | 50 | N/A | 50 | 100 |

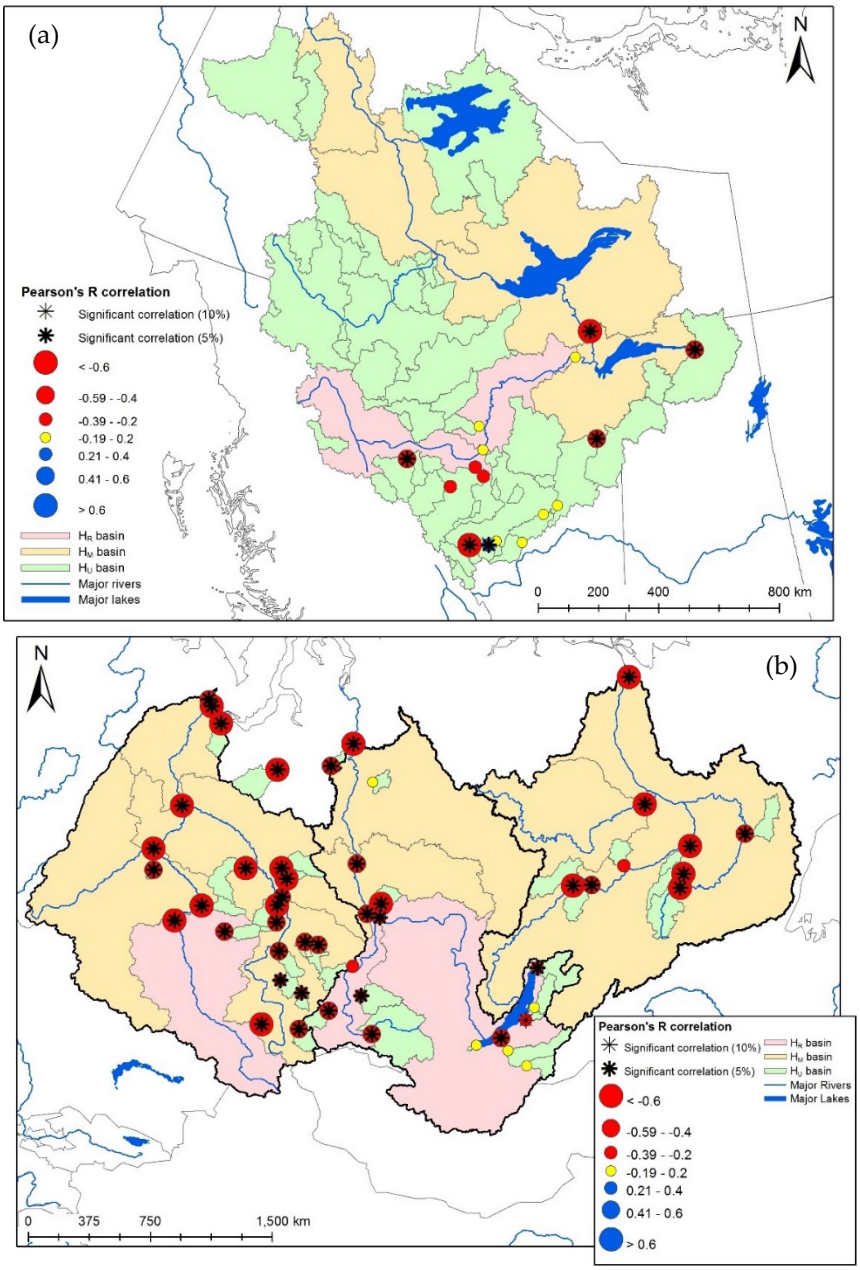

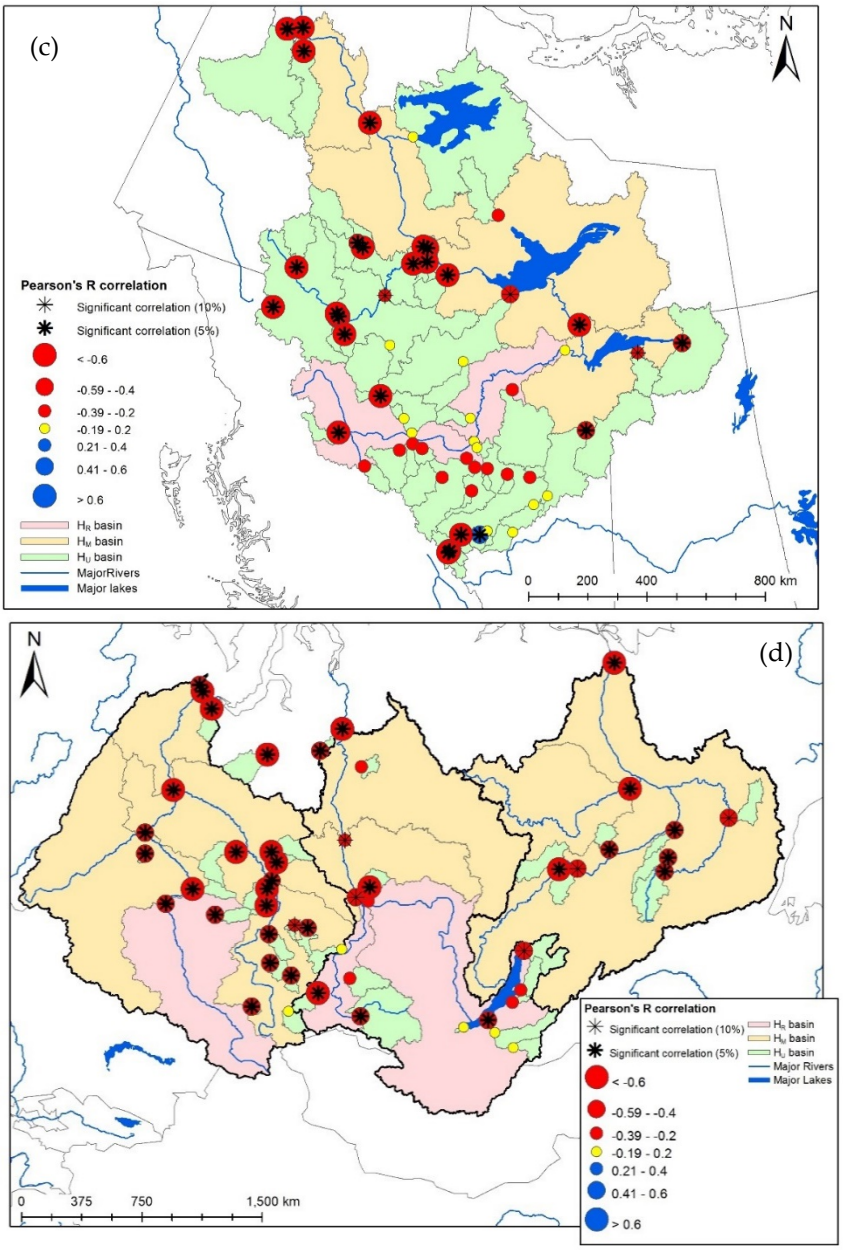


**Figure 5.** Pulse date correlations with April through June average temperature during the 1962–2000 (**a**,**b**) and 1980–2000 (**c**,**d**) periods. A negative (red) correlation indicates that a higher spring temperature corresponds with earlier pulse dates and vice versa, while a positive (blue) correlation indicates that a higher spring temperature corresponds with later pulse dates and vice versa.

Correlations of average April–June temperatures with freshet length $F_L$ during $t_1$ and $t_2$ for the Mackenzie and Asian basins are shown in Figure 6. A positive relationship indicates that warmer April–June temperatures are correlated with longer freshet length as the spring melt period is extended, and vice versa. During $t_1$, the majority of sub-basins demonstrate weak to strong positive relationships, significant at the 5% level. During $t_2$, relationships are generally weaker, with greater occurrence of non-significant or weak positive relationships when compared to $t_1$. Some negative correlations are also shown in the Mackenzie and Ob basins although relationships are still dominated by positive correlations, particularly in the southern and western high-relief regions of the Mackenzie. Similar to the analysis for $F_P$, the majority of significant correlations with $F_L$ typically occur in $H_U$ basins (Table 3).

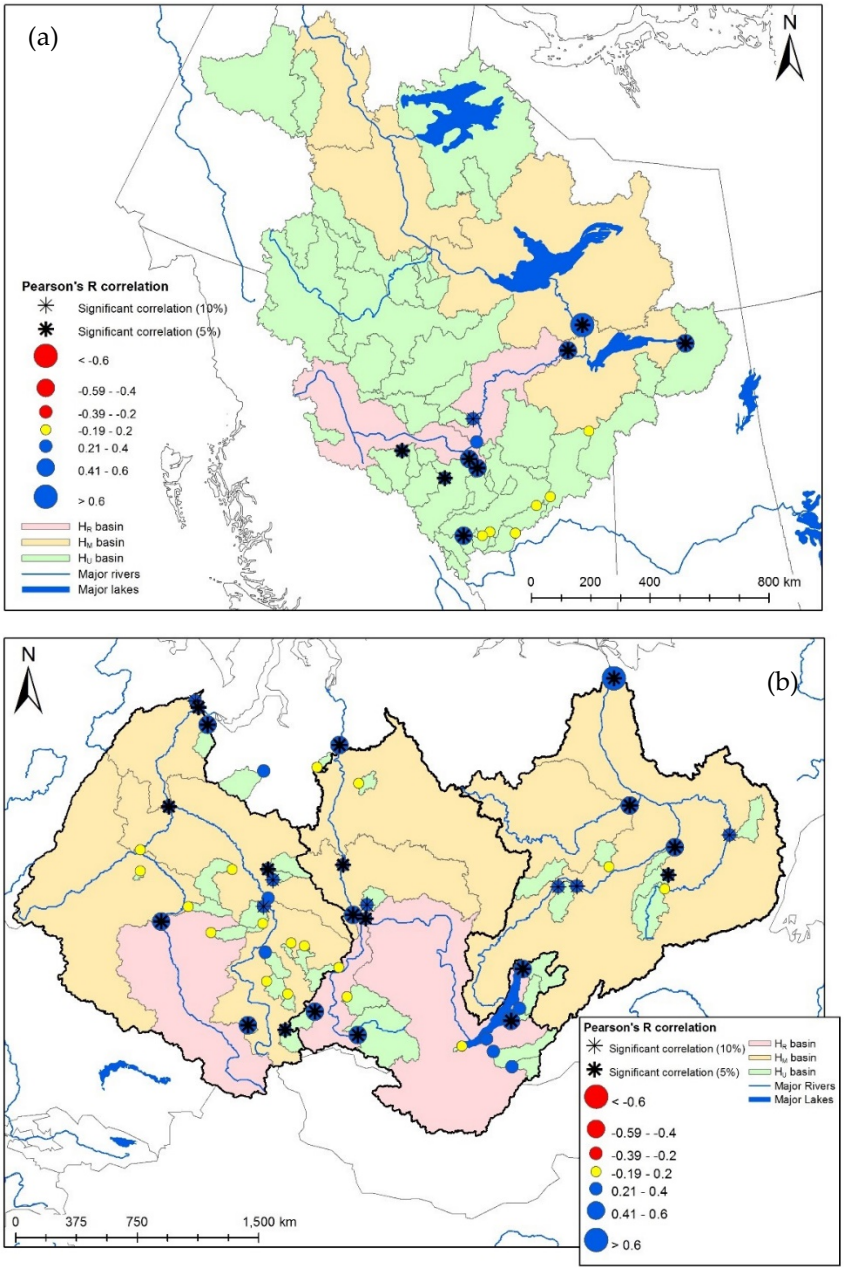
(a)
N
Pearson's R correlation
Significant correlation (10%)
Significant correlation (5%)
< -0.6
-0.59 - -0.4
-0.39 - -0.2
-0.19 - 0.2
0.21 - 0.4
0.41 - 0.6
> 0.6
$H_R$ basin
$H_W$ basin
$H_U$ basin
Major rivers
Major lakes
0 200 400 800 km
(b)
N
Pearson's R correlation
Significant correlation (10%)
Significant correlation (5%)
< -0.6
-0.59 - -0.4
-0.39 - -0.2
-0.19 - 0.2
0.21 - 0.4
0.41 - 0.6
> 0.6
$H_R$ basin
$H_W$ basin
$H_U$ basin
Major Rivers
Major Lakes
0 375 750 1,500 km

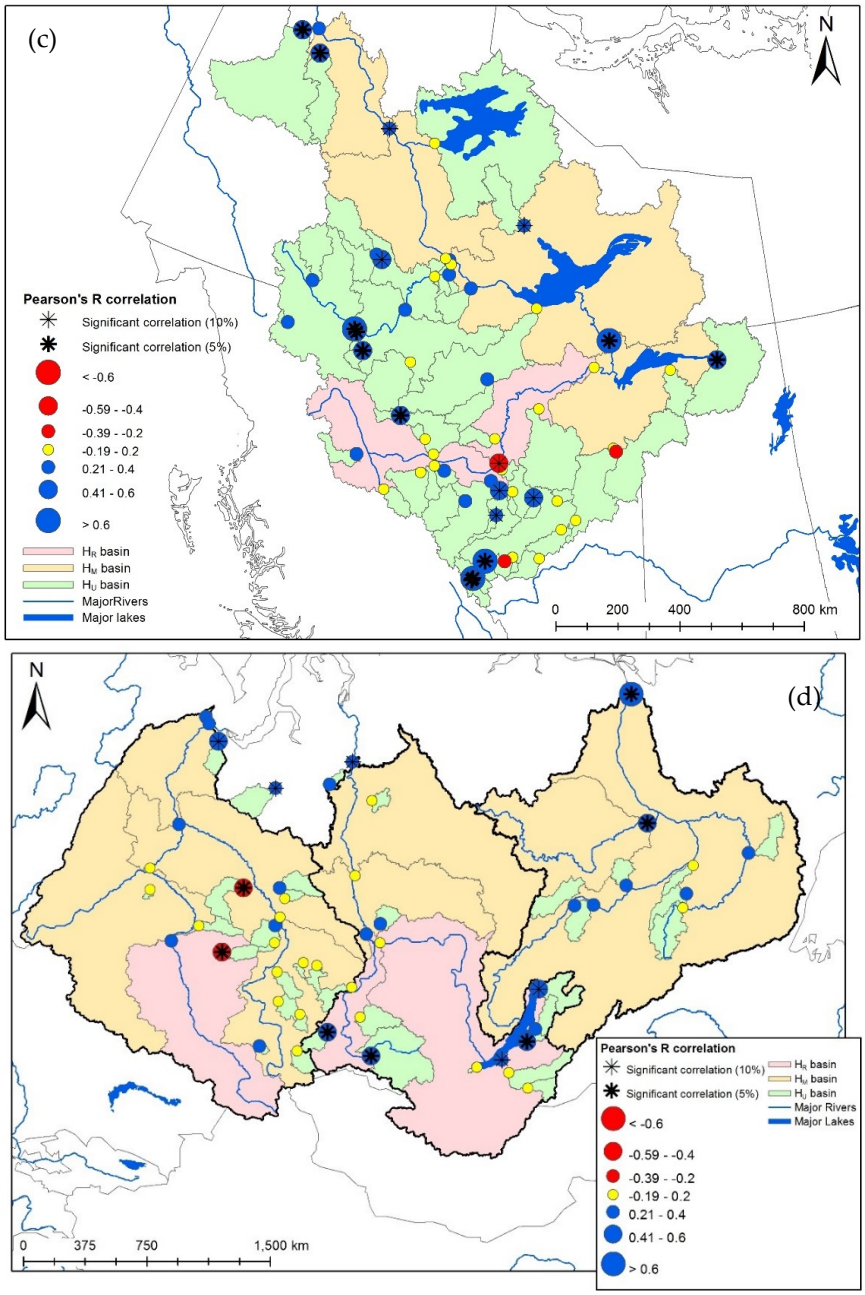


**Figure 6.** Correlation of freshet length ($F_L$) with April through June average temperature during the 1962–2000 (**a**,**b**) and 1980–2000 (**c**,**d**) periods for the Mackenzie and Asian stations. A negative (red) correlation indicates that a higher spring temperature corresponds with shorter freshet length and vice versa, while a positive (blue) correlation indicates that a higher spring temperature corresponds with longer freshet length and vice versa.

Correlations of average April–June temperatures with peak freshet magnitude $F_M$ during $t_1$ and $t_2$ for the Mackenzie and Asian basins are shown in Figure 7. A negative relationship indicates that warmer April–June temperatures are correlated with a lower peak freshet magnitude, and vice versa. During both $t_1$ and $t_2$, negative correlations are prevalent in the Mackenzie and Ob basins, with many significant at the 5% level, although correlations are generally weak to moderate. This may be indicative of a more moderated annual runoff regime, in which cold season flows are increased while spring peaks are decreased in magnitude but extended in duration. The Lena and Yenisei basins exhibit very few significant correlations in either time period, and most are negligible or weak. Relationships are strongest in the southern and western Mackenzie regions during $t_2$, with

the regulated Peace tributary indicating a significant relationship in both time periods. However, the majority of significant correlations again occur in $H_U$ basins, as given in Table 3. No significant correlations occur in any $H_R$-classified Asian sub-basin during $t_2$.

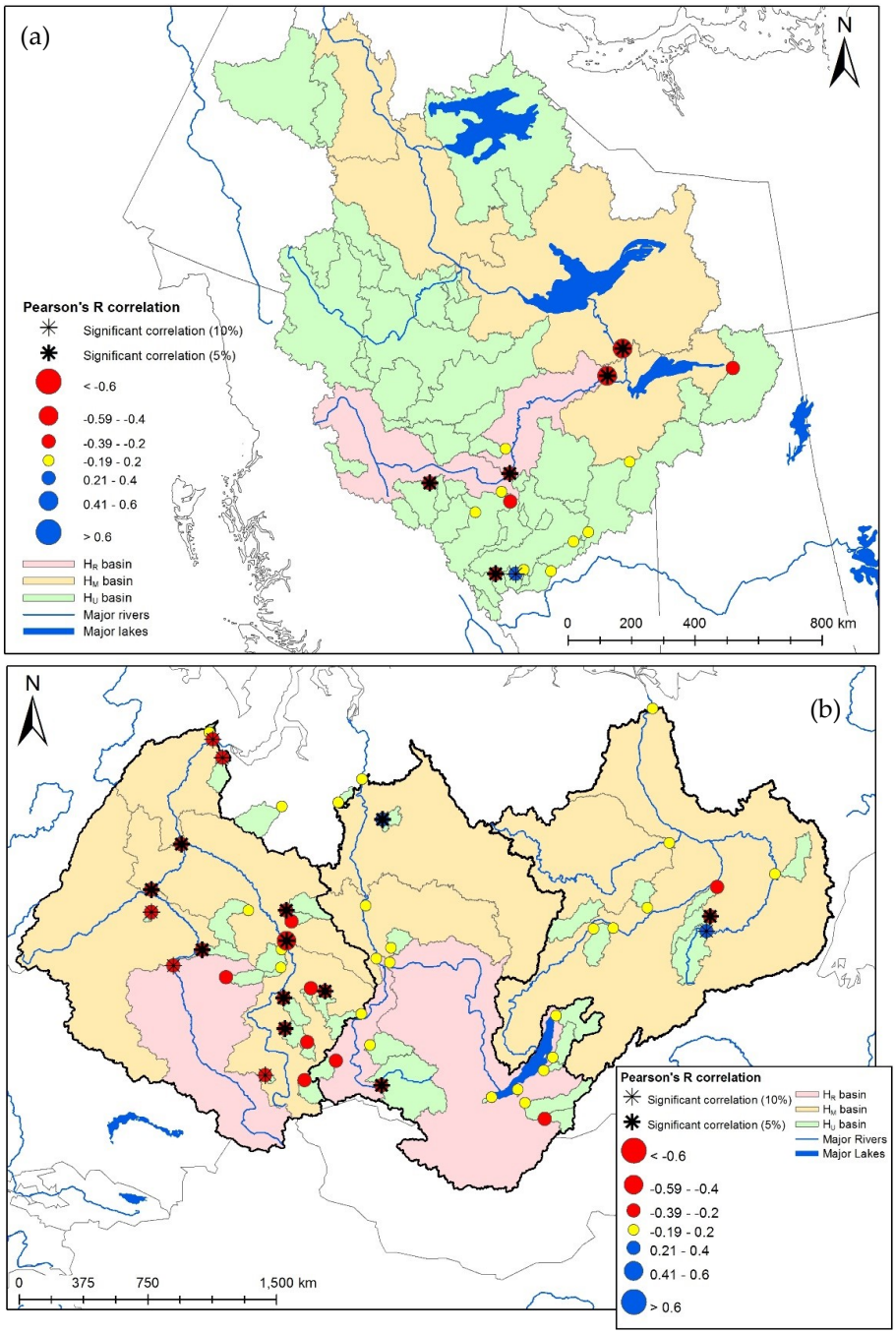

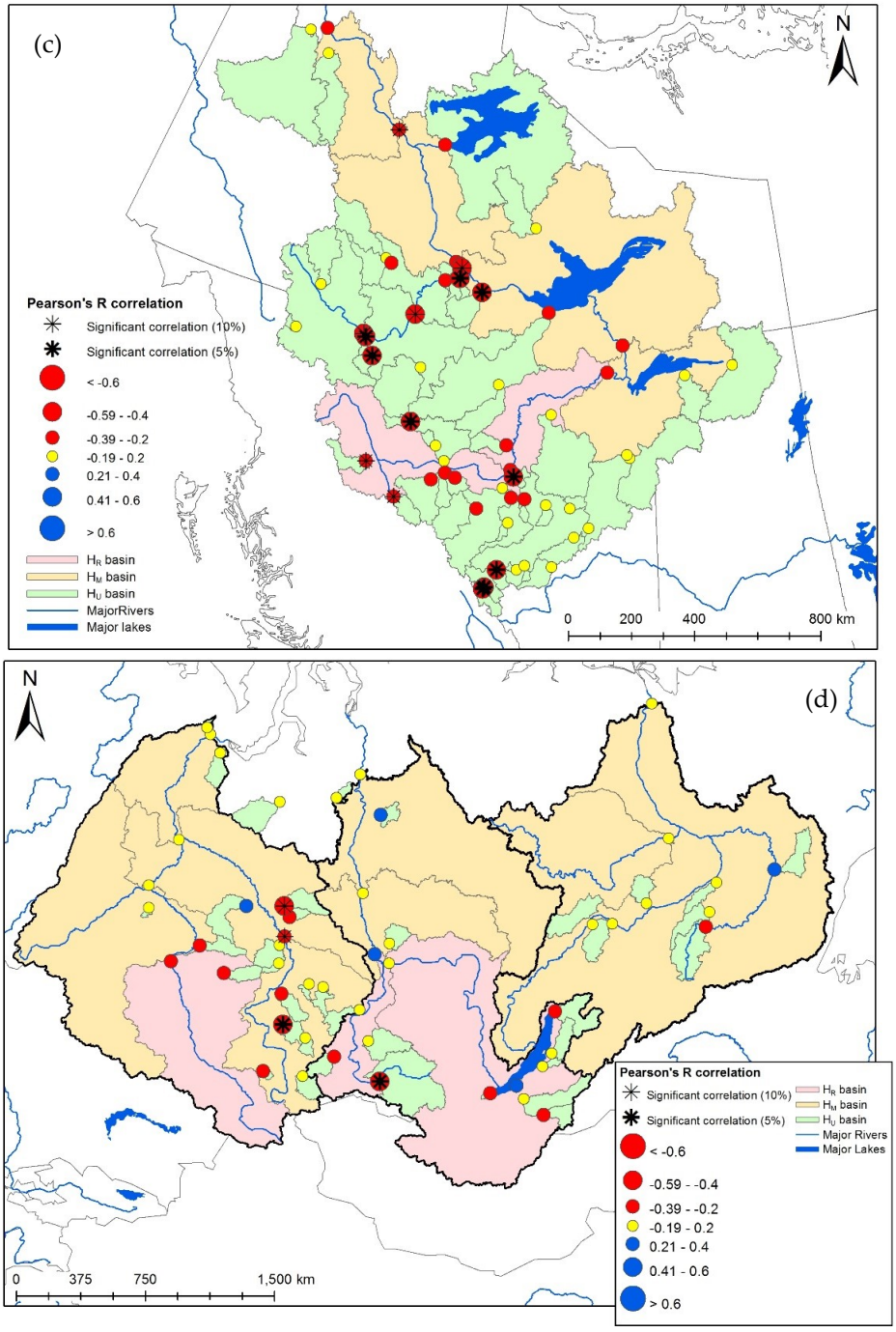


**Figure 7.** Peak freshet magnitude correlations with April–June average temperature for Mackenzie and Asian stations during the 1962–2000 (**a**,**b**) and 1980–2000 (**c**,**d**) periods. A negative (red) correlation indicates that a higher spring temperature corresponds with lower peak freshet magnitude and vice versa, while a positive (blue) correlation indicates that a higher spring temperature corresponds with higher peak freshet magnitude and vice versa.

Figure 8 provides the correlations of cumulative November–March precipitation with freshet volume $V_2$ during $t_1$ and $t_2$ for the Mackenzie and Asian basins. A positive relationship indicates that higher cumulative November–March precipitation is correlated with a higher freshet volume, and vice versa. During $t_1$, the southern Mackenzie basin, and the northern and eastern regions of the Ob and Yenisei basins, are dominated by weak to strong positive correlations significant at the 5% level. Relationships in the southern portions of the Eurasian basins are less distinct, with the majority of basins demonstrating a negligible correlation value. During $t_2$, the southern Mackenzie basin and

northern regions of the Eurasian basins again show a greater incidence of positive correlations, although the strength and significance of these relationships are generally weaker compared to $t_1$. In addition, all basins show a greater occurrence of negative correlations (particularly in the high-relief eastern Ob and western Yenisei) although none of these correlations are significant at the 5% or 10% levels. The notable regional differences in freshet volume correlations with winter precipitation suggest potential changes in hydrologic regime for some basins; this is further discussed in Section 3.5. Between 50%–100% of all significant (5%) correlations occur in $H_U$ basins during both time periods.

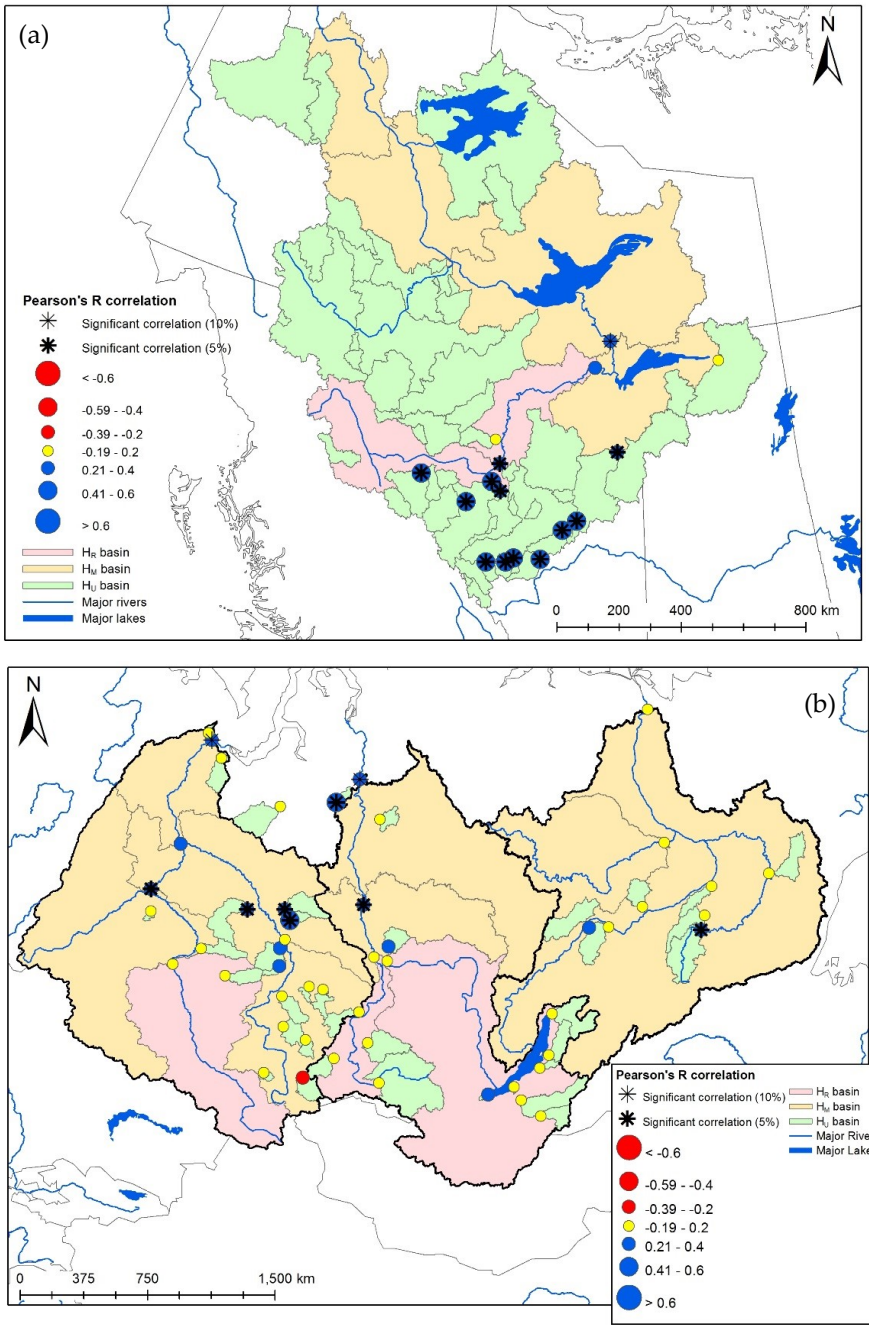

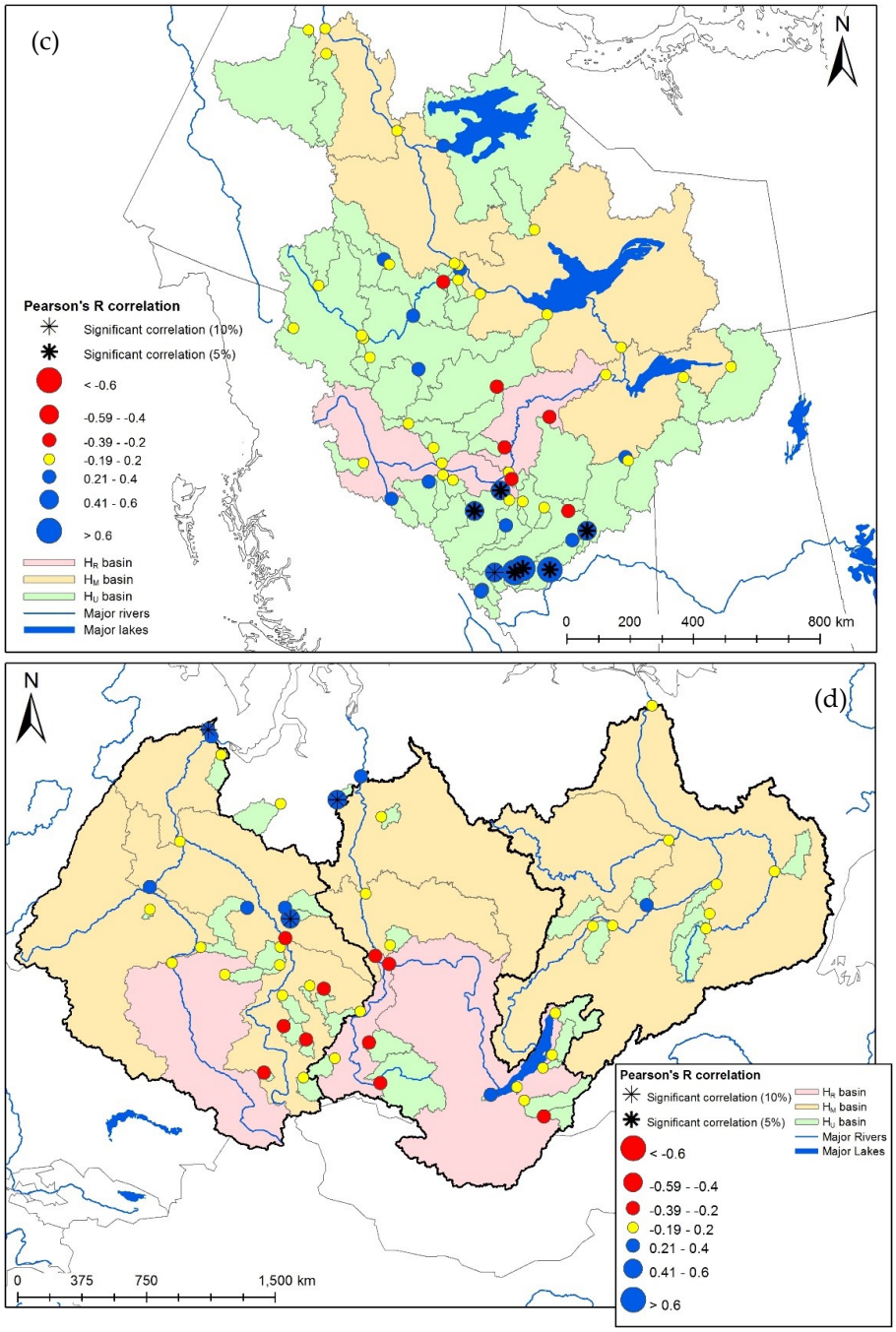


**Figure 8.** Freshet volume correlations with November–March cumulative precipitation during the 1962–2000 (**a**,**b**) and 1980–2000 (**c**,**d**) periods for Mackenzie and Asian stations. A negative (red) correlation indicates that a higher winter precipitation corresponds with lower freshet volume and vice versa, while a positive (blue) correlation indicates that a higher winter precipitation corresponds with higher freshet volume and vice versa.

Similarly, Figure 9 gives the correlations of winter precipitation with freshet volume $V_1$ (April–July cumulative volume) for the Mackenzie and Eurasian basins during $t_1$ and $t_2$. Spatial distribution of correlations in $V_1$ and $V_2$ are very similar during their respective time periods, with significant, positive relationships more prevalent in the southern Mackenzie, and the northern and eastern Yenisei and Ob basins. Significant relationships of volume $V_1$ or $V_2$ with cumulative cold season precipitation largely occur in $H_U$ basins (Table 3). No significant results are seen in any $H_R$ basin during $t_2$.

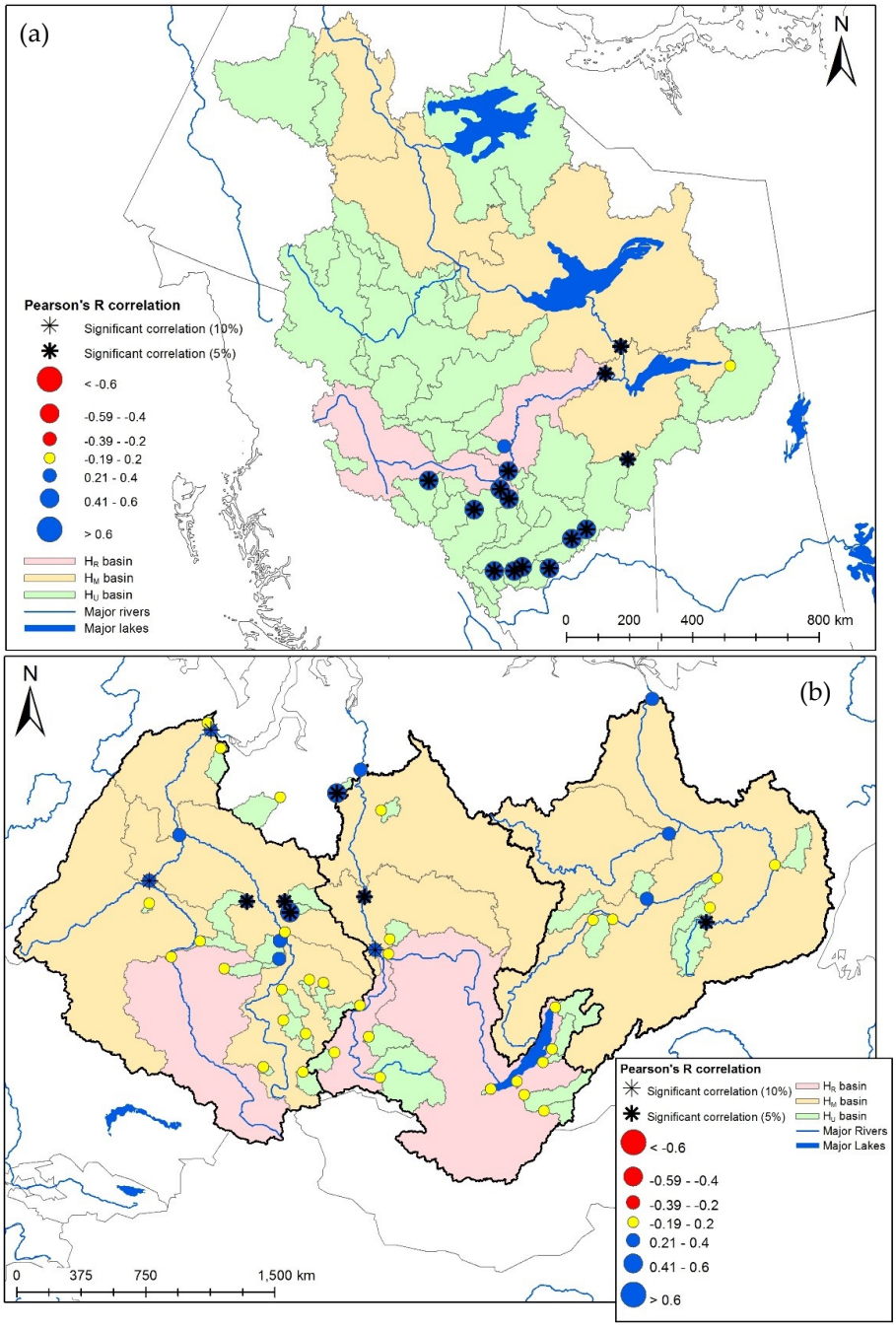
(a)
N
Pearson's R correlation
Significant correlation (10%)
Significant correlation (5%)
< -0.6
-0.59 - -0.4
-0.39 - -0.2
-0.19 - 0.2
0.21 - 0.4
0.41 - 0.6
> 0.6
$H_R$ basin
$H_M$ basin
$H_U$ basin
Major rivers
Major lakes
0 200 400 800 km
N
(b)
Pearson's R correlation
Significant correlation (10%)
Significant correlation (5%)
< -0.6
-0.59 - -0.4
-0.39 - -0.2
-0.19 - 0.2
0.21 - 0.4
0.41 - 0.6
> 0.6
$H_R$ basin
$H_M$ basin
$H_U$ basin
Major Rivers
Major Lakes
0 375 750 1,500 km

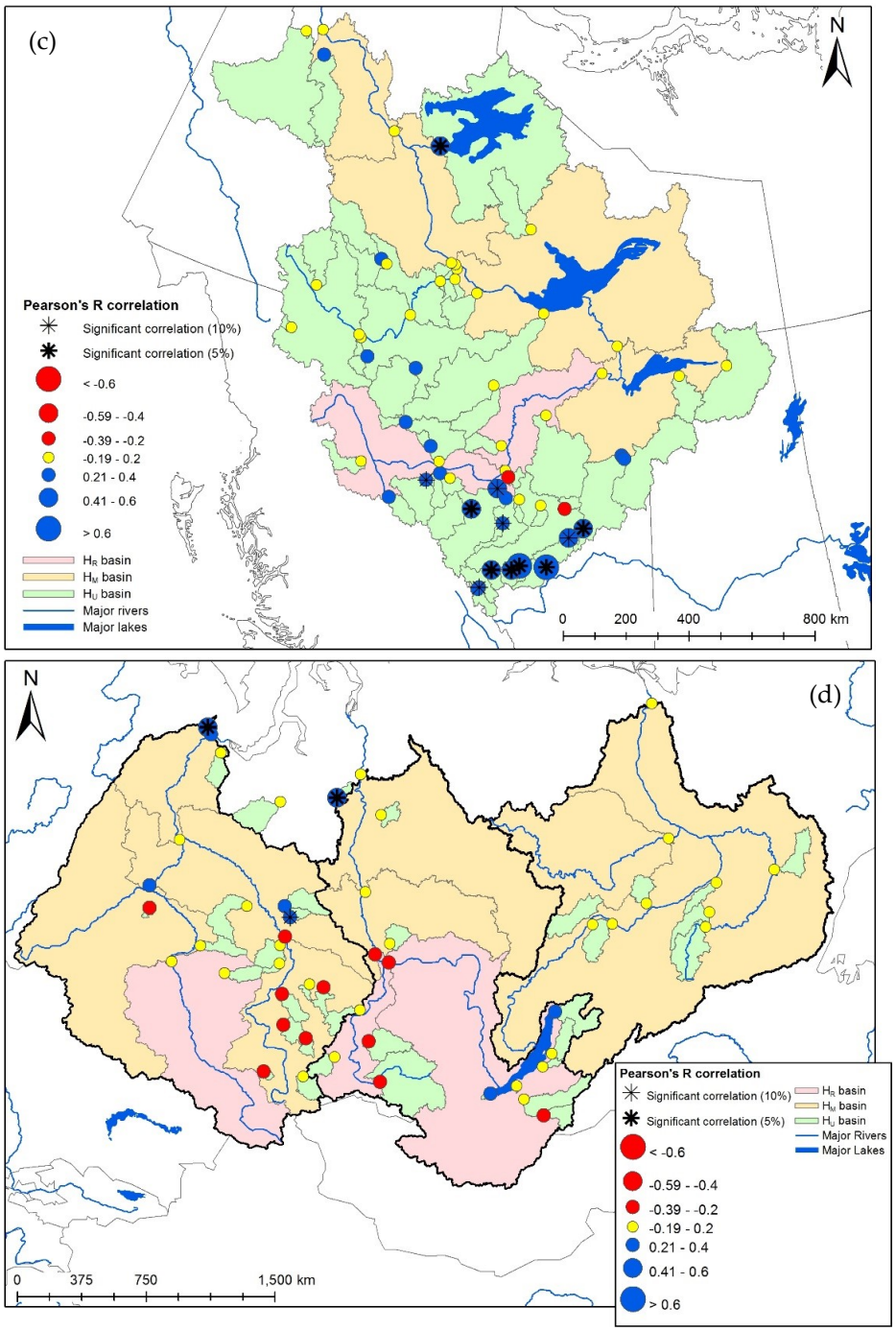


**Figure 9.** April through July volume correlations with November through March cumulative precipitation during the 1962–2000 (**a**,**b**) and 1980–2000 (**c**,**d**) periods for Mackenzie and Asian stations. A negative (red) correlation indicates that a higher winter precipitation corresponds with lower freshet volume and vice versa, while a positive (blue) correlation indicates that a higher winter precipitation corresponds with higher freshet volume and vice versa.

### *4.2. Effect of Teleconnections*

Similar to climatic drivers, the majority of significant teleconnections to most freshet measures are largely limited to $H_U$ basins, with the exception of a few instances in the regulated Irtish tributary and southern Yenisei main channel. Figure 10 presents the statistically significant March–May teleconnections with freshet pulse dates $F_P$ during $t_2$ (corresponding results for $t_1$ are provided in Figure S1 of the supplementary material). During this period, there were few significant teleconnections with NAO. AO in its negative phase

was largely associated with later occurrence of pulse dates (5 or more days) in northern Ob and Yenisei, although it was also related to earlier pulse dates in two eastern Yenisei basins. In the Mackenzie basin, the positive phase of AO was associated with earlier pulse dates. These results were consistent with descriptions of SAT anomalies during the positive phase of AO, discussed in Section 2.4. PDO was generally linked with later pulse dates in the western Mackenzie, central Siberian Plateau and eastern Yenisei in its positive phase, while in its negative phase relationships with earlier pulse dates were mostly seen in the Ob basin. This is somewhat unexpected since positive PDO is linked with positive SAT anomalies in all basins, which would generally lead to earlier pulse dates. These results may be in part due to small sample sizes, and also due to the decadal nature of PDO. Here, the $t_2$ period covers an entirely positive PDO regime, which explains the high bias towards significant relationships with positive phases. El Niño conditions were connected with earlier pulse dates in the Mackenzie and later pulse dates in Eurasia, although few significant relationships were found. These results were again consistent with SAT anomalies associated with El Niño.

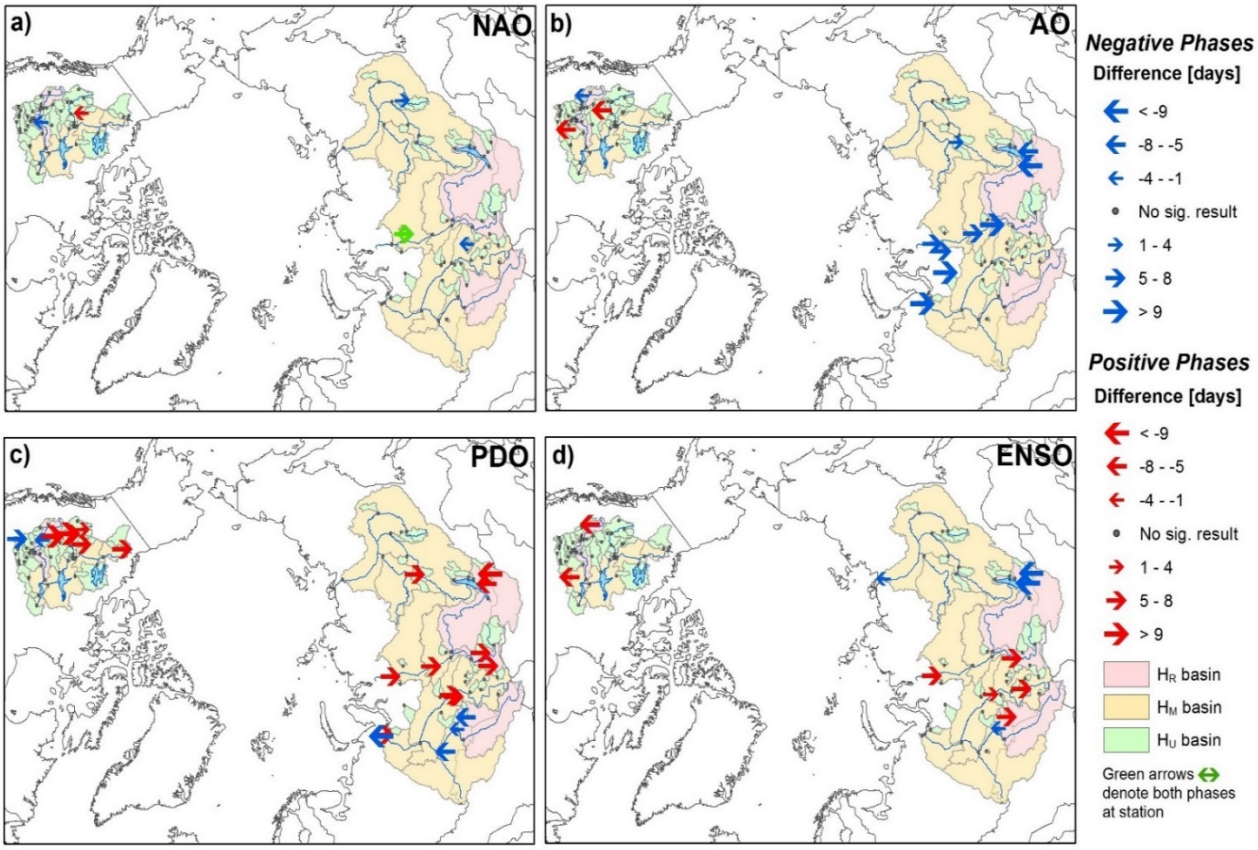


**Figure 10.** Teleconnection relationships between March through May (**a**) North Atlantic Oscillation (NAO) (**b**) Arctic Oscillation (AO) (**c**) Pacific Decadal Oscillation (PDO) and (**d**) El Niño-Southern Oscillation (ENSO) and freshet pulse dates $F_P$ during the 1980–2000 period. Blue arrows indicate that $F_P$ is affected by the negative phase of a teleconnection index while red arrows indicate that $F_P$ is affected by the positive phase of the index at a 5% significance level. The direction of the arrows indicates whether $F_P$ is delayed (pointing right) or advancing (pointing left) while the size of the arrow represents the magnitude.

The March–May teleconnections with peak freshet magnitude $F_M$ during $t_2$ are presented in Figure 11 (corresponding results for $t_1$ are provided in Figure S2 of the supplementary material). During this period, positive NAO associated with higher SAT anomalies demonstrated linkages with lower peak freshet magnitude, especially in the eastern Ob, although AO relationships did not persist in Eurasian basins. During the latter period, negative AO leading to lower Mackenzie basin winter precipitation anomalies (i.e., drier

winter conditions) largely demonstrated relationships with decreased $F_M$ in the northern and eastern Mackenzie basin. Significant relationships with PDO were limited to its negative phase during $t_2$, showing that, for the most part, negative PDO associated with cooler winter temperatures as well as somewhat drier winter conditions (albeit with regional variation) had significant relationships with decreased freshet magnitude. ENSO revealed strong relationships in both phases in the Mackenzie sub-basins, with a distinct separation of phases visible between lower and middle latitudes. As discussed in Section 2.4, there is indeed a division between the north-western and south-eastern portions of the Mackenzie basin, whereby El Niño conditions lead to wetter winters in the former and drier winters in the latter, and vice versa for La Niña. Here, La Niña (cooler, drier winters in the upper region) showed strong relationships with decreased $F_M$ in the upper Mackenzie while El Niño (warmer, drier winters in the southern region) was similarly connected to decreased $F_M$ in the southern Mackenzie.

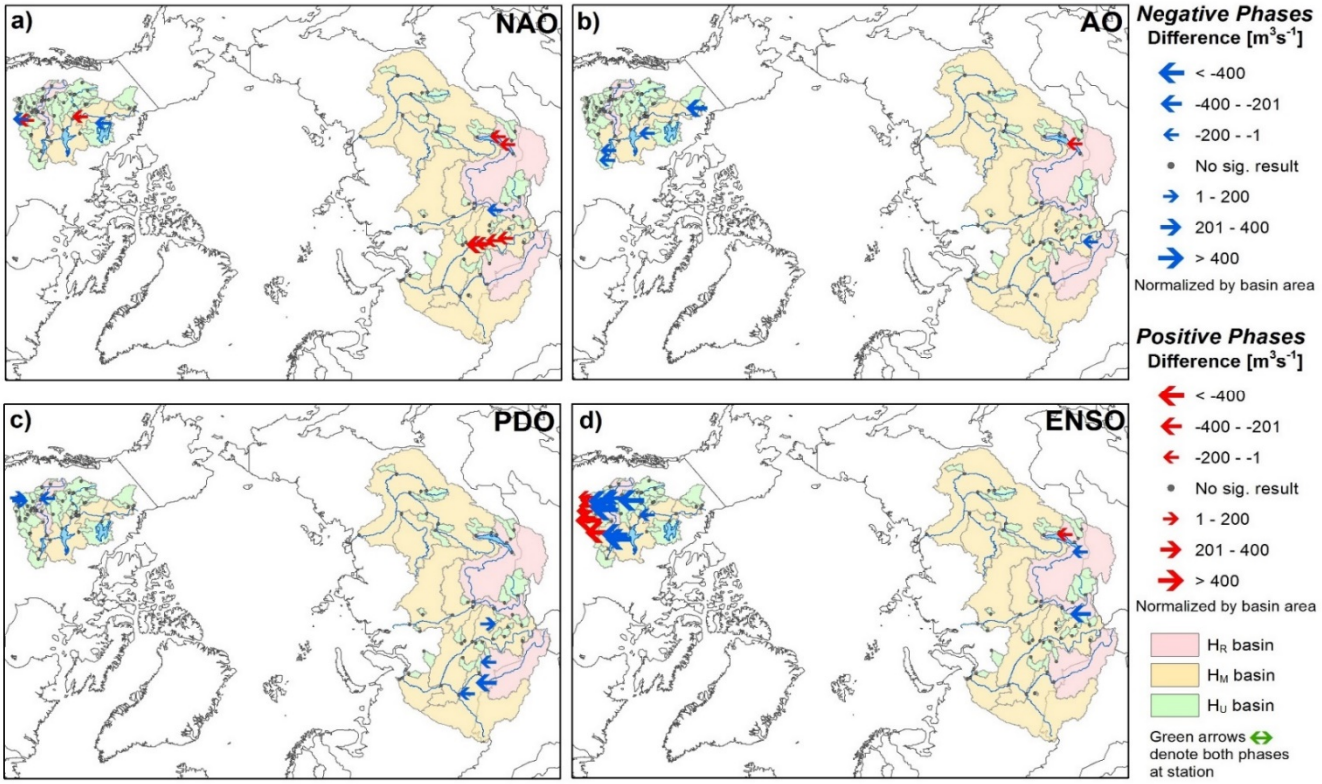


**Figure 11.** Teleconnection relationships between March through May (**a**) NAO (**b**) AO (**c**) PDO and (**d**) ENSO and peak freshet magnitude $F_M$ during the 1980–2000 period. Blue arrows indicate that $F_M$ is affected by the negative phase of a teleconnection index while red arrows indicate that $F_M$ is affected by the positive phase of the index at a 5% significance level. The direction of the arrows indicates whether $F_M$ is increasing (pointing right) or decreasing (pointing left) while the size of the arrow represents the magnitude.

Distributions of December–February teleconnections with freshet volume are similar for $V_1$ and $V_2$ during their respective time periods. The December–February teleconnections with freshet volume $V_2$ during $t_2$ are presented in Figure 12 (corresponding results for $t_1$ are provided in Figure S3 of the supplementary material). In most cases, positive phases of AO and NAO are generally linked with decreased freshet volumes mostly in the eastern Yenisei. Despite positive AO and NAO typically leading to wetter winter conditions, freshet volume may be adversely affected due to correspondingly higher winter temperatures resulting in lower snowpack accumulation. PDO and ENSO demonstrated stronger relationships with $V_2$, particularly in the southern Mackenzie basin. Negative PDO (drier winter conditions over much of the Mackenzie basin) was associated with decreased freshet volumes, although we recall that $t_2$ falls mostly in a positive PDO regime.

Similar to how positive AO and NAO resulting in warmer winter temperatures may lead to less winter snowpack accumulation, El Niño conditions are also strongly associated with decreased volumes in the southern Mackenzie basin. In Eurasia, positive PDO (associated with generally drier winters in the Ob basin and wetter winters in the Yenisei) are related to decreased freshet volumes in several Ob sub-basins and increased volumes in one Yenisei sub-basin.

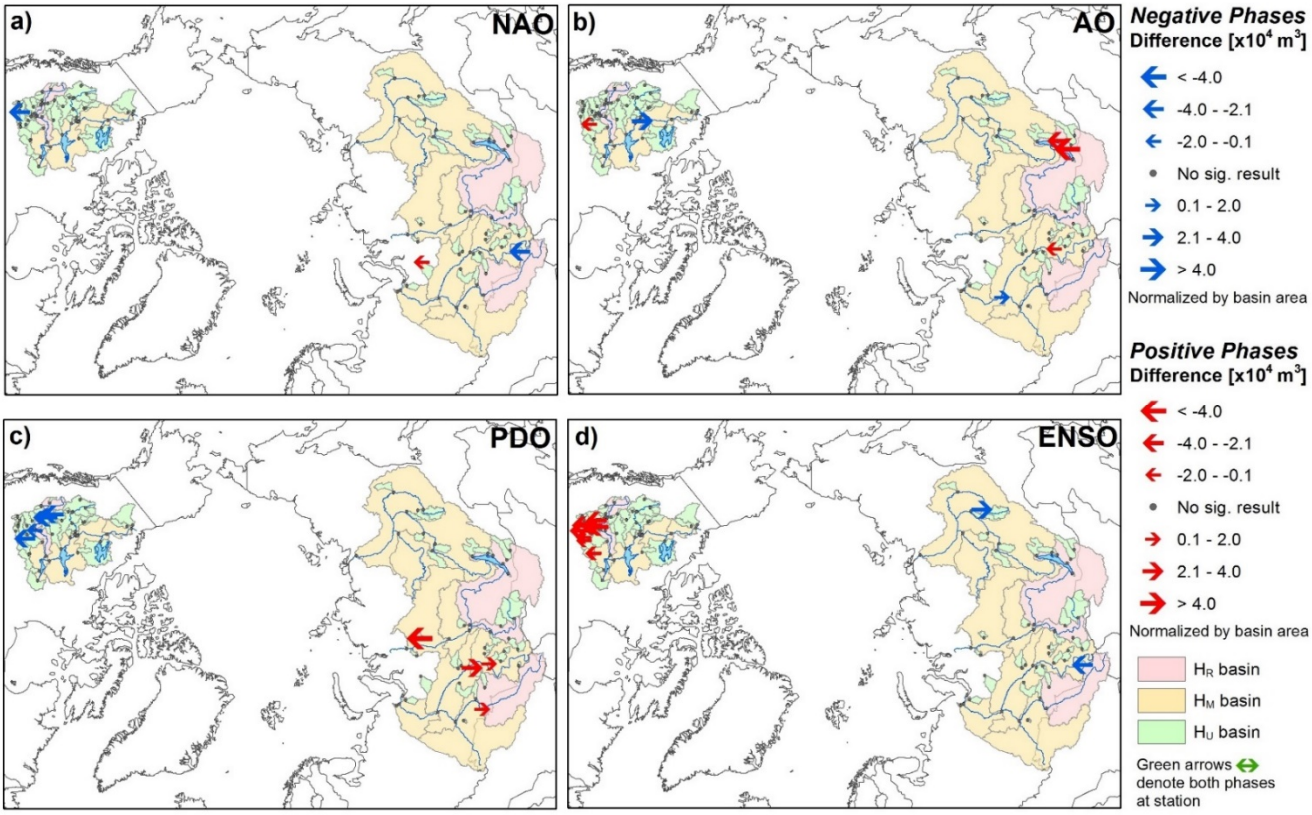


**Figure 12.** Teleconnection relationships between December through February (**a**) NAO (**b**) AO (**c**) PDO and (**d**) ENSO and freshet volume $V_2$ during the 1980–2000 period. Blue arrows indicate that $V_2$ is affected by the negative phase of a teleconnection index while red arrows indicate that $V_2$ is affected by the positive phase of the index at a 5% significance level. The direction of the arrows indicates whether $V_2$ is increasing (pointing right) or decreasing (pointing left) while the size of the arrow represents the magnitude.

## 5. Summary

Correlations of spring temperature with freshet measures $F_P$, $F_L$ and $F_M$ were typically stronger and had more significant results when compared to correlations of cold-season precipitation with freshet volumes $V_1$ and $V_2$, particularly in the Asian basins where few significant precipitation–volume correlations existed. Correlations in the Mackenzie basin were largely marked by strong regional similarities in the southern and western high-relief drainage areas, with fewer patterns evident in the low-relief northern and eastern regions. Correlation patterns in the Asian basins were less clear, with the strongest clustering appearing in the higher-relief areas of the southern Ob, and southern, western and eastern Yenisei basin. Pulse dates were strongly negatively correlated with April–June temperature in most sub-basins, with the majority of these being statistically significant. This indicated that warmer spring temperatures were associated with an earlier freshet onset in those basins. Pulse date correlations in the Mackenzie basin were exclusively limited to $H_M$ and $H_U$ sub-basins. In the Asian basins, significant correlations and trends were also found in $H_R$ sub-basins, suggesting that flow regulation does not have a substantial impact on pulse timing in those regions. Freshet length showed mostly positive correla-

tions throughout all basins during 1962–2000, indicating that warmer April–June temperatures are correlated with sustained snow melt and a longer freshet period. However, during 1980–2000, relationships were generally weaker, with some sub-basins showing negative correlations with freshet length. Many of those mixed results occurred in lowland regions with limited topographical relief, suggesting that basins with less high-elevation snow storage were more susceptible to decreased freshet duration with warmer spring temperatures. Significant correlations and trends are also found in $H_R$ sub-basins, suggesting again that flow regulation does not strongly affect the natural relationship of temperature with timing measures.

Peak freshet magnitude $F_M$ displayed mostly negative correlations with spring temperatures in the Mackenzie, Ob and Yenisei basins during both time periods. This revealed that warmer spring temperatures resulted in decreased peak freshet magnitudes in those regions, with some notable exceptions particularly in the Lena basin during $t_2$ where peak freshet magnitudes were largely increasing. The analysis revealed that the combination of generally more persistent freshet durations and lower freshet magnitudes resulted in an overall flattening of the annual hydrograph shape in many sub-basins. This may also have been indicative of a potential shift from a distinctly nival hydrological regime to a more hybrid or even a pluvial regime in some basins. Freshet volume ($V_1$ and $V_2$) correlations with winter precipitation showed distinct regional variation in all basins, where higher winter precipitation in the southern alpine region of the Mackenzie and northern regions of the Asian basins was positively correlated with freshet volumes that showed increasing trends. However, in the southern Ob and western Yenisei basins, higher winter precipitation did not necessarily result in greater freshet volumes. This was evidenced by weaker or even negative correlations, possibly due to susceptibility to a warming climate causing a shift to a more rainfall-driven hydrologic regime. This indicates that the integrated effects of increased temperature and precipitation may have resulted in less winter snowpack precipitation accumulation and correspondingly lower freshet volumes. Interestingly, volume correlations with winter precipitation were strongest in the southern Mackenzie region, likely as a result of upstream regulation along the Peace River tributary whose drainage area encompasses these smaller regions. In Asian basins, no strong correlations were found in any $H_R$ basin during 1980–2000. This suggests that extensive regulation in the Asian basins may be obscuring the impact of climatic controls in those regions.

Relationships between freshet measures and the different teleconnection indices revealed that regional patterns were generally less consistent during the shorter period of $t_2$ compared to $t_1$, most likely due to smaller sample sizes. Where statistically significant relationships existed, only one phase of the teleconnection has typically dominated the relationship although there were a few occasions where significant correlations were found in both phases with opposite response. Positive AO and NAO leading to warmer winters and springs were typically associated with earlier pulse dates, decreased peak freshet magnitude and lower freshet volume although there were some regional exceptions. Positive ENSO (El Niño), associated with positive SAT and precipitation anomalies over the Mackenzie and negative SAT and precipitation anomalies over the Eurasian basins (with some regional variability), corresponded with earlier Mackenzie and later Eurasian pulse dates, and decreased peak freshet magnitude in the southern Mackenzie basin. El Niño had strong associations with decreased freshet volume in the southern Mackenzie but had little effect on Eurasian basins. Meanwhile, positive PDO, associated with positive SAT anomalies and mixed, mostly positive precipitation anomalies in all basins, tended to coincide with later pulse dates and lower freshet magnitudes in all basins. These unexpected relationships of PDO with delayed pulse onset may be due to the long-term decadal variation of this index, particularly during $t_2$ which occurs entirely in a warm PDO phase. Similarly, a warm phase of PDO was associated with decreased freshet volume in the Mackenzie basin during $t_1$ but not during $t_2$. Further research is suggested to obtain more

insight into these PDO interactions, as well as the potential integrated effects of multiple teleconnection indices.

## 6. Conclusions

The study assesses the large-scale atmospheric and surface climatic conditions affecting the magnitude, timing and regional variability of the spring freshets within sub-basins of the four largest Arctic-draining watersheds (MOLY). Freshets timing, duration and peak magnitude ($F_P$, $F_L$ and $F_M$) are found to be strongly linked to spring temperatures. Regulation did not appear to completely suppress these climatic relationships, since significant correlations existed, regardless of regulation status. Regulation did, however, appear to limit climatic relationships of cold season precipitation with freshet volume $V_1$ and $V_2$, since few significant correlations with volume were found in regulated stations. This reinforces the notion that flow impoundment does act to suppress the effects of some natural climatic drivers of freshet generation, with potential impact on seasonal runoff regimes. However, volume relationships with cold season precipitation were not as distinct as temperature linkages with freshet timing, even for the unregulated basins. This suggests that an integrated multi-variable approach incorporating both temperature and precipitation is needed to further clarify these freshet volume relationships.

Sub-basin freshet measures are also significantly related to several large-scale climatic teleconnection patterns. However, since there were significant differences in climatic and large-scale atmospheric variability relationships with unregulated stations versus those stations incorporating an upstream regulation signal, the effects of flow regulation on the timing and magnitude of freshet response needs to be more fully evaluated. Future research should also look into this via hydraulic flow modelling that can remove the effect of regulation and thereby permit the controlling signals of climate to be better identified. Likewise, flow modelling can be used to determine whether regulation can actually mitigate the effects of climatic variation on discharge seasonality and magnitude at the outlets. This will allow for further discussion on the regional impacts of climatic influences on overall circumpolar freshwater contribution to the Arctic Ocean. This discussion is especially important since climate change, resulting in an increase in precipitation and air temperature over Arctic basins, as well as a potential increase in extreme climatic events such as stronger El Niños, will continue to alter the nature of terrestrial freshwater contribution to the Arctic Ocean.

**Supplementary Materials:** The following are available online at www.mdpi.com/2073-4441/13/2/179/s1, Table S1: Characteristics of drainage sub-basins identified in Figure 2. Note: M = Mackenzie, O = Ob, L = Lena, Y = Yenisei, $H_U$ = unregulated, $H_R$ = Regulated and $H_M$ = minimally regulated. Stations IDs in *italic* have data during $t_2$ (1980–2000) only; Figure S1: Teleconnection relationships between March through May a) NAO b) AO c) PDO and d) ENSO and freshet pulse dates $F_P$ during the 1962–2000 period. Blue arrows indicate $F_P$ is affected by the negative phase of a teleconnection index while red arrows indicates $F_P$ is affected by the positive phase of the index at a 5% significance level. The direction of the arrows indicate whether $F_P$ is delayed (pointing right) or advancing (pointing left) while the size of the arrow represents the magnitude; Figure S2. Teleconnection relationships between March through May (a) NAO (b) AO (c) PDO and (d) ENSO and peak freshet magnitude $F_M$ during the 1962–2000 period. Blue arrows indicate $F_M$ is affected by the negative phase of a teleconnection index while red arrows indicates $F_M$ is affected by the positive phase of the index at a 5% significance level. The direction of the arrows indicate whether $F_M$ is increasing (pointing right) or decreasing (pointing left) while the size of the arrow represents the magnitude; Figure S3. Teleconnection relationships between December through February (a) NAO (b) AO (c) PDO and (d) ENSO and freshet volume $V_2$ during the 1962–2000 period. Blue arrows indicate $V_2$ is affected by the negative phase of a teleconnection index while red arrows indicates $V_2$ is affected by the positive phase of the index at a 5% significance level. The direction of the arrows indicate whether $V_2$ is increasing (pointing right) or decreasing (pointing left) while the size of the arrow represents the magnitude.

**Author Contributions:** Conceptualization, R.A., T.P., Y.D. and B.B.; Methodology, R.A., Y.D. and B.B.; Data analysis, R.A. Original draft preparation, R.A. and Y.D.; Review and editing, R.A. and T.P., Y.D. and B.B. All the authors review the manuscript prior to and during the submission process to the Water MDPI Journal. All authors have read and agreed to the published version of the manuscript.

**Funding:** This work was partially supported by a Discovery Grant and ArcticNet funding from the Natural Sciences and Engineering Council of Canada (NSERC) to one of the co-authors.

**Institutional Review Board Statement:** Not applicable.

**Informed Consent Statement:** Not applicable.

**Data Availability Statement:** Not applicable.

**Acknowledgments:** This work was partially supported by a Discovery Grant and ArcticNet funding from the Natural Sciences and Engineering Council of Canada (NSERC). The authors would also like to acknowledge the Arctic Rapid Integrated Monitoring System (ArcticRIMS), the Regional Hydrometeorological Data Network for the Pan-Arctic Region (R-ArcticNet), the European Centre for Medium-Range Weather Forecasts, and the National Oceanic and Atmospheric Administration for freely providing data.

**Conflicts of Interest:** The authors declare no conflict of interest. The funders had no role in the design of the study; in the collection, analyses, or interpretation of data; in the writing of the manuscript, or in the decision to publish the results.

## References

1. Aagaard, K.; Carmack, E.C. The role of fresh water in ocean circulation and climate. *J. Geophys. Res.* **1989**, *94*, 14485–14498, doi:10.1029/JC094iC10p14485.
2. Carmack, E.C. The freshwater budget of the Arctic Ocean: Sources, storage and sinks. In *The Freshwater Budget of the Arctic Ocean*; Lewis, E.L., Jones, E.P., Lemke, P., Prowse, T.D., Wadhams, P., Eds.; Kluwer: Dordrecht, The Netherlands, 2000; pp. 91–126.
3. Serreze, M.C.; Francis, J.A. The Arctic Amplification Debate. *Clim. Chang.* **2006**, *76*, 241–264, doi:10.1007/s10584-005-9017-y.
4. Peterson, B.J.; Holmes, R.M.; McClelland, J.W.; Vörösmarty, C.J.; Lammers, R.B.; Shiklomanov, A.I.; Shiklomanov, I.A.; Rahmstorf, S. Increasing river discharge to the Arctic Ocean. *Science* **2002**, *298*, 2171–2173.
5. Arnell, N.W. Implications of climate change for freshwater inflows to the Arctic Ocean. *J. Geophys. Res. Atmos.* **2005**, *110*, D07105.
6. Prowse, T.D.; Flegg, P.O. Arctic river flow: A review of contributing areas. In *The Freshwater Budget of the Arctic Ocean*; Lewis, E.L., Jones, E.P., Lemke, P., Prowse, T.D., Wadhams, P., Eds.; Kluwer: Dordrecht, The Netherlands, 2000; pp. 269–280.
7. Kattsov, V.M.; Walsh, J.E.; Chapman, W.L.; Govorkova, V.; Pavlova, T.V.; Zhang, X. Simulation and Projection of Arctic Freshwater Budget Components by the IPCC AR4 Global Climate Models. *J. Hydrometeorol.* **2007**, *8*, 571–589.
8. McClelland, J.W.; Holmes, R.M.; Dunton, K.H.; Macdonald, R.W. The Arctic Ocean Estuary. *Estuaries Coasts* **2011**, *35*, 353–368.
9. Lammers, R.B.; Shiklomanov, A.I.; Vörösmarty, C.J.; Fekete, B.M.; Peterson, B.J. Assessment of contemporary Arctic river runoff based on observational discharge records. *J. Geophys. Res.* **2001**, *106*, 3321–3334.
10. Prowse, T.; Bring, A.; Mård, J.; Carmack, E. Arctic freshwater synthesis: Introduction. *J. Geophys. Res. Biogeosci.* **2015**, *120*, 2121–2131.
11. Bring, A.; Fedorova, I.; Dibike, Y.; Hinzman, L.; Mård, J.; Mernild, S.H.; Prowse, T.; Semenova, O.; Stuefer, S.L.; Woo, M.K. Arctic terrestrial hydrology: A synthesis of processes, regional effects, and research challenges. *J. Geophys. Res. Biogeosci.* **2016**, *121*, 621–649.
12. McPhee, M.G.; Proshutinsky, A.; Morison, J.H.; Steele, M.; Alkire, M.B. Rapid change in freshwater content of the Arctic Ocean. *Geophys. Res. Lett.* **2009**, *36*, L10602.
13. Grabs, W.E.; Portmann, F.; De Couet, T. Discharge observation networks in Arctic regions: Computation of the river runoff into the Arctic Ocean, its seasonality and variability. In *The Freshwater Budget of the Arctic Ocean*; Lewis, E.L., Jones, E.P., Lemke, P., Prowse, T.D., Wadhams, P., Eds.; Kluwer: Dordrecht, The Netherlands, 2000; pp. 249–267.
14. Ahmed, R. Spatio-Temporal Variation in the Spring Freshet of Major Circumpolar Arctic River Systems. Master's Thesis, University of Victoria, Victoria, BC, Canada, 4 July 2015.
15. Ahmed, R.; Prowse, T.; Dibike, Y.; Bonsal, B.; O'Neil, H. Recent Trends in Freshwater Influx to the Arctic Ocean from Four Major Arctic-Draining Rivers. *Water* **2020**, *12*, 1189.
16. Finnis, J.; Cassano, J.; Holland, M.; Uotila, P. Synoptically forced hydroclimatology of major Arctic watersheds in general circulation models, Part 1: The Mackenzie River Basin. *Int. J. Climatol.* **2009**, *29*, 1226–1243.
17. Yang, D.; Ye, B.; Shiklomanov, A. Discharge characteristics and changes over the Ob River watershed in Siberia. *J. Hydrometeorol.* **2004**, *5*, 595–610.
18. Yang, D.; Kane, D.L.; Hinzman, L.D.; Zhang, X.; Zhang, T.; Ye, H. Siberian Lena River hydrologic regime and recent change. *J. Geophys. Res.* **2002**, *107*, 4694.

19. Yang, D.; Ye, B.; Kane, D.L. Streamflow changes over Siberian Yenisei river basin. *J. Hydrol.* **2004**, *296*, 59–80.
20. Dyurgerov, M.B.; Carter, C.L. Observational Evidence of Increases in Freshwater Inflow to the Arctic Ocean. *Arct. Antarct. Alp. Res.* **2004**, *36*, 117–122.
21. Loeng, H.; Brander, K.; Carmack, E.; Denisenko, S.; Drinkwater, K.; Hansen, B.; Kovacs, K.; Livingston, P.; Mclaughlin, F.; Bellerby, R.; et al. Chapter 9: Marine Systems. In *Arctic Climate Impact Assessment*; Symon, C., Arris, L., Heal, B., Eds.; Cambridge University Press: New York, NY, USA, 2005; pp. 453–538.
22. Nuttall, M. (Ed.) *Encyclopedia of the Arctic*; Routledge: Abingdon, UK, 2005.
23. Woo, M.; Thorne, R. Streamflow in the Mackenzie basin, Canada. *Arctic* **2003**, *56*, 328–340.
24. Lydolph, P.E.; Temple, D.; Temple, D. *Geograhpy of the U.S.S.R.*; Wiley: New York, NY, USA, 1977.
25. Stuefer, S.; Yang, D.; Shiklomanov, A. Effect of streamflow regulation on mean annual discharge variability of the Yenisei River. In *Cold Region Hydrology in a Changing Climate, Proceedings of the Symposium H02 Held during IUGG2011, Melbourne, Australia, 28 June to 7 July 2011*; IAHS Publications: Oxfordshire, UK, 2011; Volume 346, pp. 27–32.
26. Serreze, M.C. Arctic Climate. In *Encyclopedia of Atmospheric Sciences*; Holton, J.R., Curry, J.A., Pyle, J.A., Eds.; Academic Press: Cambridge, MA, USA, 2003; p. 171.
27. Trenberth, K. The definition of El Nino. *Bull. Am. Meteorol. Soc.* **1997**, *78*, 2771–2777.
28. Mantua, N.J.; Hare, S.R.; Zhang, Y.; Wallace, J.M.; Francis, R.C. A Pacific interdecadal climate oscillation with impacts on salmon production. *Bull. Am. Meteorol. Soc.* **1997**, *78*, 1069–1079.
29. Thompson, D.W.J.; Wallace, J.M. The Arctic Oscillation signature in the wintertime geopotential height and temperature fields. *Geophys. Res. Lett*. **1998**, *25*, 1297–1300.
30. Hurrell, J.W. Decadal trends in the North Atlantic Oscillation: Regional temperatures and precipitation. *Science* **1995**, *269*, 676–679.
31. Bonsal, B.R.; Prowse, T.D.; Duguay, C.R.; Lacroix, M.P. Impacts of large-scale teleconnections on freshwater-ice break/freeze-up dates over Canada. *J. Hydrol.* **2006**, *330*, 340–353.
32. Déry, S.; Stieglitz, M.; McKenna, E.; Wood, E.F. Characteristics and trends of river discharge into Hudson, James, and Ungava Bays, 1964–2000. *J. Clim.* **2005**, *18*, 2540–2557.
33. Hamlet, A.F.; Lettenmaier, D.P. Columbia River streamflow forecasting based on ENSO and PDO climate signals. *J. Water Resour. Plan. Manag*. **1999**, *125*, 333–341.
34. Neal, E.G.; Walter, M.T.; Coffeen, C. Linking the Pacific Decadal Oscillation to seasonal stream discharge patterns in Southeast Alaska. *J. Hydrol.* **2002**, *263*, 188–197.
35. Ye, H.; Yang, D.; Zhang, T.; Zhang, X.; Ladochy, S.; Ellison, M. The impact of climatic conditions on seasonal river discharges in Siberia. *J. Hydrometeorol.* **2004**, *5*, 286–295.
36. Serreze, M.C.; Bromwich, D.H.; Clark, M.P.; Etringer, A.J.; Zhang, T.; Lammers, R. Large-scale hydro-climatology of the terrestrial Arctic drainage system. *J. Geophys. Res.* **2002**, *108*, 8160.
37. Stoner, A.M.K.; Hayhoe, K.; Wuebbles, D.J. Assessing General Circulation Model Simulations of Atmospheric Teleconnection Patterns. *J. Clim.* **2009**, *22*, 4348–4372.
38. Kingston, D.G.; Lawler, D.M.; McGregor, G.R. Linkages between atmospheric circulation, climate and streamflow in the northern North Atlantic: Research prospects. *Prog. Phys. Geogr.* **2006**, *30*, 143–174.
39. Rogers, A.N.; Bromwich, D.H.; Sinclair, E.N.; Cullather, R.I. The atmospheric hydrologic cycle over the Arctic basin from reanalyses, Part 2. *J. Clim.* **2001**, *14*, 2414–2429.
40. Sveinsson, O.G.; Lall, U.; Gaudet, J.; Kushnir, Y.; Zebiak, S.; Fortin, V. Analysis of climatic states and atmospheric circulation patterns that influence Québec spring streamflows. *J. Hydr. Eng.* **2008**, *13*, 411–425.
41. R-ArcticNET. A Regional Hydrometeorological Data Network for Russia. Available online: http://www. https://www.r-arcticnet.sr.unh.edu/v4.0/index.html (accessed on 11 December 2019).
42. Jones, P.; Harris, I. *CRU TS3. 21: Climatic Research Unit (CRU) Time-Series (TS) Version 3.21 of High Resolution Gridded Data of Month-by-Month Variation in Climate (Jan. 1901–Dec. 2012*); NCAS British Atmospheric Data Centre: Leeds, UK, 2013.
43. Gibson, J.J.; Prowse, T.D.; Peters, D.L. Hydroclimatic controls on water balance and water level variability in Great Slave Lake. *Hydrol. Process.* **2006**, *20*, 4155–4172.
44. Cayan, D.R.; Kammerdiener, S.A.; Dettinger, M.D.; Caprio, J.M.; Peterson, D.H. Changes in the Onset of Spring in the Western United States. *Bull. Am. Meteorol. Soc.* **2001**, *82*, 399–415.
45. Stewart, I.; Cayan, D.; Dettinger, M. Changes toward earlier streamflow timing across western North America. *J. Clim.* **2005**, *18*, 1136–1155.
46. Maurer, E.P.; Lettenmaier, D.P.; Mantua, N.J. Variability and potential sources of predictability of North American runoff. *Water Resour. Res.* **2004**, *40*, W09306.
47. Burn, D.H. Climatic influences on streamflow timing in the headwaters of the Mackenzie River Basin. *J. Hydrol.* **2008**, *352*, 225–238.